Planetary Volcanology Field Trip
Pinacate Volcanic Field
Sonora, Mexico

PINACATE FIELD TRIP STUDENT EXERCISE QUESTION SHEETS

Name _____

GLG 490/598 Field Trip to the Pinacate Volcanic Field

Sarah A. Fagents, David A. Williams, Ronald Greeley, and John F. McHone

INTRODUCTION

This is a 2 d field trip to the Pinacate Biosphere Reserve in Sonora, Mexico. The Pinacate volcanic field has been active for the past 2–3 m.y. Lavas are derived from melting of deep, garnet-bearing asthenosphere, possibly as a miniplume that welled up near, but distinct from, a spreading center in the adjacent Gulf of California (Sea of Cortez) to the south (Goss et al., 2008). The Pinacate field contain diverse volcanic landforms, including a shield volcano, a tuff cone, maars, cinder cones, and lava flows. Two different alkalic rock series are represented: One constitutes the >400 monogenetic cones and craters formed over the last 1.2 m.y. or more; the other forms the extinct Santa Clara shield volcano. The former consists of basalts and hawaiites, whereas the latter constitutes an entire alkaline differentiation series: basalt, hawaiite, mugearite, benmoreite, and trachyte.

This trip will focus on the deposits and morphologic expressions of explosion craters, volcanic cones, and lava flows.

Guidebook Cover Image: The Pinacate volcanic field as imaged by the Spaceborne Imaging Radar-C/X-band Synthetic Aperture Radar (SIR-C/X-SAR) carried onboard the space shuttle *Endeavor* on 18 April 1994. Image is centered at 31.84°N, 113.47°W. The colors are assigned to different radar frequencies and polarizations of the radar as follows: red is L band (23.5 cm), horizontally transmitted and received; green is L band, horizontally transmitted, vertically received; and blue is C band (4–8 cm), horizontally transmitted, vertically received. National Aeronautics and Space Administration (NASA) photojournal image PIA 01852.

DAY 1

Mile 0	**Depart Tempe:** Head south on Rural Road to Broadway Road.
Mile 1	Turn right on Broadway.
Mile 3.5	At the junction with I-10, head south toward Tucson for ~8.5 miles.
Mile 12	Take the Maricopa road exit and head south for 29 miles.
Mile 43	At the junction with Hwy 84, turn west.
Mile 49	Take I-8 west.
	Stop 1. Rest area (or Gila Bend). Overview of geology of the area.
Mile 83	Take exit 116 at Gila Bend, turn south on Hwy 85.
Mile 126?	**Stop 2.** Mining pit in Ajo. Discussion of mineral deposits and mining operations. **Mile 160?**
Stop 3	(optional) Organ Pipe National Monument visitor center.
Mile 163	**Stop 4.** Mexican border at Lukeville. After crossing, proceed to Sonoyta.
Mile 165	Turning right onto Route 8, heading southwest towards Puerto Peñasco. The oldest volcanic center (Volcan Santa Clara) of the Pinacate volcanic field will become visible to the west.

EXERCISE 1. Remote sensing of the Pinacate region.

En route to the Pinacate volcanic field, examine the color SIR-C/X-SAR radar image of the volcanic field (the front cover of your field guide). Based on your understanding of how microwave radiation interacts with surface materials, together with what you see from the van, suggest answers to the following questions:

1.1 What are the anastamosing channels in the southeast portion of the image? What causes the bright radar return?

_____

1.2 What might compose the broad, dark patterned surface in the far southwest of the image?

_____

1.3 What causes the reddish hues in the image?

_____

1.4 Within the main volcanic area, how many prominent (>500 m diameter) craters can you identify? Comment on the variations in morphology and crater floor brightness/color.

1.5 What are the lobate, bright yellowish features prominent in the eastern part of the field? What is the cause of their radar brightness?

Now examine the false-color Landsat image of the Pinacate volcanic field (Fig. 1). This was constructed with band 7 (2.08–2.35 μm), band 4 (0.76–0.90 μm), and band 2 (0.52–0.60 μm) in the red, green, and blue channels, respectively. By referring to Figure 2, which shows spectra of common rocks and minerals, answer the following questions.

1.6 What are the abundant circular red features? Why are they red?

1.7 Note that many of the craters and other features that are prominent in the radar image are less distinct in visible to near infrared wavelengths. Why is much of the volcanic field dark?

1.8 What is the material making up the yellowish surface to the southwest?

Mile 200 At the sign for the Pinacate Biosphere Reserve, turn right off Route 8 onto dirt road, stop at visitor's center to register and obtain a camping permit. Continue north on the dirt road for ~10 mi (~16.1 km).
Mile 210 Bear left at fork in road, following the sign to Crater Elegante.
Mile 217 **Stop 6.** Crater Elegante. Lunch.

Crater Elegante is ~1600 m in diameter and 244 m deep, and it formed some 32,000 yr ago. The rim affords a great perspective of the surrounding geology: Volcan Santa Clara dominates the southwestern horizon. To the northeast, there are the cones of Tecolote, Mayo, and Cerro Colorado. The low-lying area to the south hosts abundant small cones. Lava flows are clearly visible to the west and northeast.

EXERCISE 2. Crater Elegante.

Walk up to the crater rim and (with caution) scramble a few meters down the slope toward the crater floor to examine the outcrops.

2.1 Describe the deposits in terms of their components, bedding structures, dip, etc.

2.2 What eruption mechanism do these deposits represent?

Walk west along the crater rim for 500–1000 m. Look across to the highest point along the rim on the opposite side.

2.3 What do you notice about the structure in the opposite wall?

Now backtrack and walk east around the crater toward the highest point. Along the way, note the relief of the crater rim in relation to the surrounding area, the dip of the beds, and the depth to crater floor. Also note the variety of large ejecta types.

2.4 Describe the material comprising the highest point of the rim. How does it differ from that found elsewhere? What is the relationship of this structure to the crater?

2.5 Based on everything you've observed, what type of feature is Elegante? How did it form?

2.6 Examine the enlargement of the radar image covering Elegante (Fig. 3). Explain the variation in radar brightness in the crater floor.

2.7 What features does Elegante have or lack compared to impact craters?

Returning to the vans, leave Elegante and travel north around Tecolote Cone.

Mile 221 **Stop 7.** ʻAʻā lava flow front. We will examine the lava textures and discuss the emplacement processes of ʻaʻā flows. Walk up and examine the textures of the lava surface and flow front. How do these characteristics relate to the radar brightness? Noting the characteristics of the surrounding surfaces, examine the enlarged radar image (Figs. 4, A1, A2) to locate our position.

Mile 224 **Stop 8.** Continuing along the road, we will turn left into the Tecolote campground.

EXERCISE 3. Lava flows.

Walk west along the short road through the campground for ~500 m until you enter a broad basin surrounded by thick lava flows. One flow emanates from Mayo Cone, immediately to the north of the campground; another comes from the Tecolote Cone complex to the south. Walk clockwise around the margins of the basin to examine the different lava flows.

3.1 Locate the pāhoehoe flow. Note the surface textures. What is its stratigraphic relationship and age relative to the ʻaʻā flow?

3.2 From the radar image, what can you say about the abundance of pāhoehoe flows relative to ʻaʻā in the Pinacate volcanic field?

DAY 2

EXERCISE 4. Mayo Cone.

Starting from the campground, skirt westward along the base of the Mayo Cone and head up over the saddle into the interior of the breached cone complex.

4.1 Describe the characteristics of the pyroclastic material comprising the cone's outer flanks. How does this differ from the material you saw at Elegante?

4.2 Describe the characteristics of the pyroclasts and deposits within the interior of the breached cone.

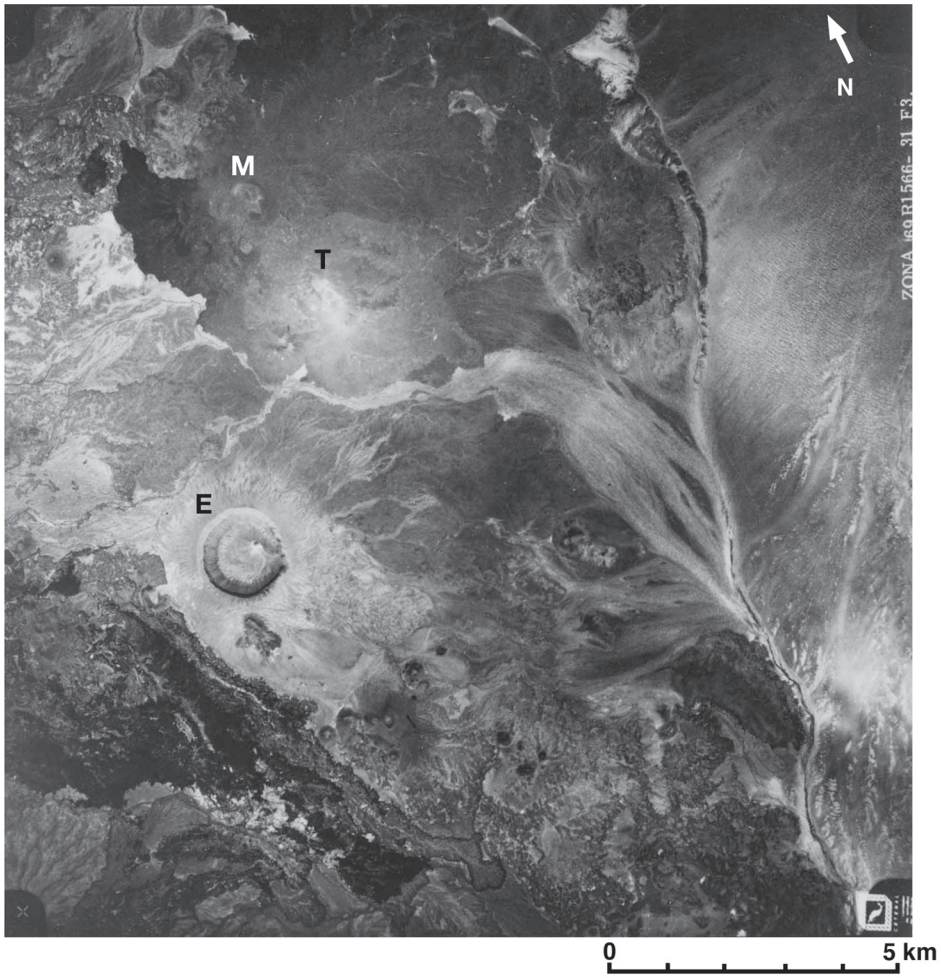

Figure A1. Aerial photo of the Pinacate volcanic field, showing Crater Elegante (E), Tecolote (T), and Mayo (M) Cones. Image is courtesy Arizona State University Space Photography Laboratory.

4.3 Based on your observations of the cone complex and pyroclastic material, describe the eruption mechanisms responsible for the deposits. How do you think the eruption evolved through time?

Returning to the vans, leave the campground and head west to Cerro Colorado.

Mile 230 **Stop 9.** View of Cerro Colorado to the north. Note the relief of the structure and dip of the bedding.
Mile 233 **Stop 10. North rim of Cerro Colorado.**

Cerro Colorado is >27,000 yr old, based on Ar/Ar dating of overlying lapilli. The crater is ~1000 m in diameter, with the crater floor lying >100 m below the highest point on the south rim. The morphology of the crater records multiple centers of activity. Note the presence of Diaz Playa to the north of Cerro Colorado.

EXERCISE 5. Cerro Colorado.

Walk down a few meters inside the crater rim onto the benches to examine rim deposits.

5.1 Describe the characteristics of these deposits (clast types, bedding, dip, etc.).

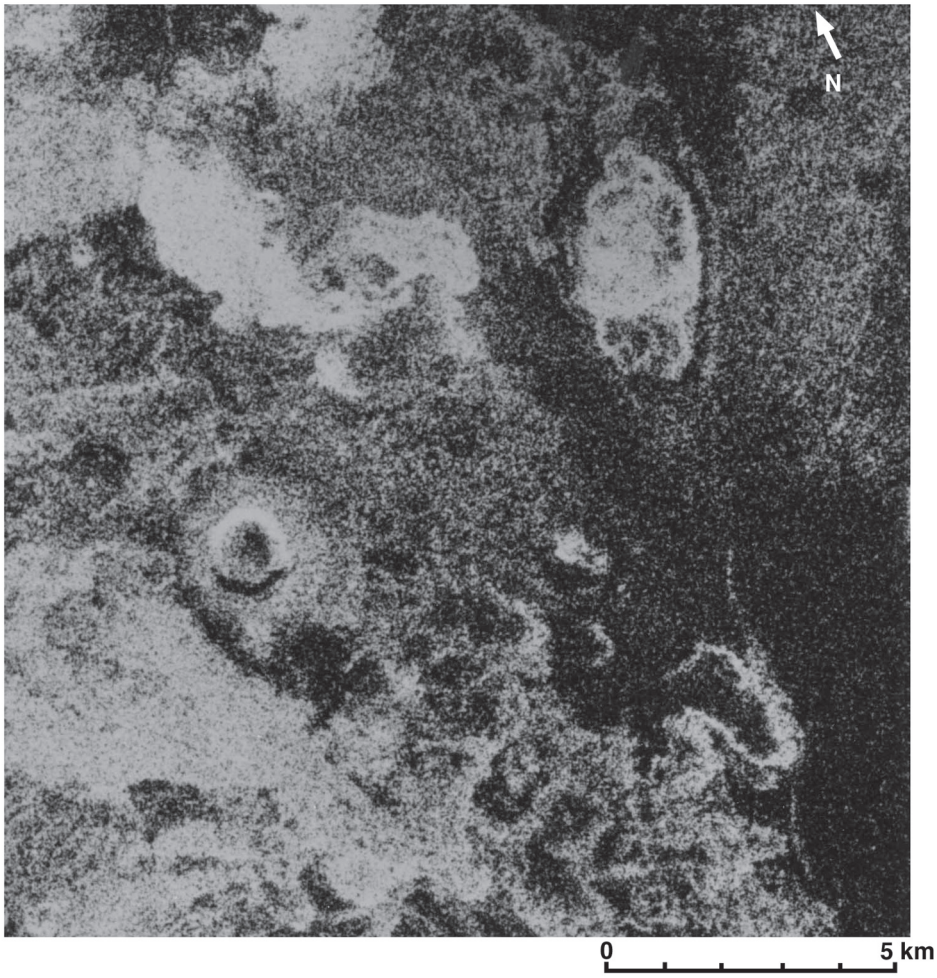

Figure A2. Spaceborne Imaging Radar (SIR)-A radar image of the Pinacate volcanic field, showing Crater Elegante, and Tecolote and Mayo Cones (cf. Fig. A1). Image is courtesy Arizona State University Space Photography Laboratory.

5.2 How were these deposits formed?

5.3 What do the lithic clasts say about the pre-eruption environment?

5.4 How do these deposits differ from those at Elegante?

Looking down into the crater, note the pinkish tan deposits exposed at the bottom of the crater's north wall. These are mudstones, which probably represent preexisting playa deposits.

5.5 What does the morphology of the crater interior suggest regarding the focus of eruptive activity?

Return to the crater rim. Walk counterclockwise around to the northwest part of the rim. Note the presence of long-wavelength radial dune forms on the outer flanks. Examine the deposits in the crater wall.

5.6 What do these deposit characteristics suggest about their mechanism of emplacement?

5.7 What do your observations of cone relief, deposit characteristics, and bedding dip suggest about eruption style and the role of external water? What type of feature is Cerro Colorado?

Return to the crater rim and head back to the vans.

5.8 Locate Cerro Colorado on the radar image (front cover). Explain the radar-dark apron.

5.9 Study the radar image to determine the locations of major craters. Given what you now know about the formation of volcanic craters at Pinacate, what inferences might you make about the paleohydrology of this region?

5.10 How might one distinguish between impact craters and volcanic craters such as Cerro Colorado and Crater Elegante in remotely sensed data?

Lunch at the vans. We will leave Cerro Colorado and head north out of the Reserve.

Mile 234 Head north through Playa Diaz.
Mile 239 Head north on cinder road.
Mile 240 Exit Pinacate Biosphere Reserve. Join Route 2 heading east.
Mile 272 Turn left at junction with Route 8. Head north through Sonoyta to border.
Mile 274 Border crossing. Reverse the outbound route to return to Tempe.

Reference Reprints Included in This Guidebook. ***(These appear courtesy of the Arizona Geological Survey.)***

Gutmann, J.T., and Sheridan, M.F., 1978, Geology of the Pinacate volcanic field, *in* Burt, D.M., and Pewe, T.L., eds., Guidebook to the Geology of Central Arizona: State of Arizona, Bureau of Geology and Mineral Technology Special Paper 2, p. 47–60.

Lynch, D.J., and Gutmann, J.T., 1987, Volcanic structures and alkaline rocks in the Pinacate volcanic field of Sonora, Mexico, *in* Davis, G.H., and VanderDolder, E.M., eds., Geologic Diversity of Arizona and its Margins: Excursions to Choice Areas: State of Arizona, Bureau of Geology and Mineral Technology Special Paper 5, p. 309–322.

OTHER USEFUL REFERENCES

Arvidson, R.E., and Mutch, T.A., 1974, Sedimentary patterns in and around craters from the Pinacate volcanic field, Sonora, Mexico: Some comparisons with Mars: Geological Society of America Bulletin, v. 85, p. 99–104, doi:10.1130/0016-7606(1974)85<99:SPIAAC>2.0.CO;2.

Bezy, J.V., Gutmann, J.T., and Haxel, G.B., 2000, A Guide to the Geology of the Organ Pipe Cactus National Monument and the Pinacate Biosphere Reserve: Tucson, Arizona Geological Survey, Down-to-Earth 9, 63 p.

Goss, A.R., Gutmann, J.T., Varekamp, J.C., and Kamenov, G., 2008, Pb isotopes and trace elements of the Pinacate volcanic field, northwestern Sonora, Mexico: A Basin and Range mini-plume near the EPR spreading center: Geological Society of America Abstracts with Programs, v. 40, no. 6, abstract 331-7 (CD-ROM).

Greeley, R., Christensen, P.R., and McHone, J.F., 1987, Radar characteristics of small craters: Implications for Venus: Earth, Moon, and Planets, v. 37, p. 89–111, doi:10.1007/BF00054327.

Gutmann, J.T., 1974, Tubular voids within labradorite phenocrysts from Sonora, Mexico: The American Mineralogist, v. 59, p. 666–672.

Gutmann, J.T., 1976, Geology of Crater Elegante, Sonora, Mexico: Geological Society of America Bulletin, v. 87, p. 1718–1729, doi:10.1130/0016-7606(1976)87<1718:GOCESM>2.0.CO;2.

Gutmann, J.T., 1977, Textures and genesis of phenocrysts and megacrysts in basaltic lavas from the Pinacate volcanic field: American Journal of Science, v. 277, p. 833–861, doi:10.2475/ajs.277.7.833.

Gutmann, J.T., 1979, Structure and eruptive cycle of cinder cones in the Pinacate volcanic field and the controls of Strombolian activity: The Journal of Geology, v. 87, p. 448–454, doi:10.1086/628432.

Gutmann, J.T., 1986, Origin of four- and five-phase ultramafic xenoliths from Sonora, Mexico: The American Mineralogist, v. 71, p. 1076–1084.

Lutz, T.M., and Gutmann, J.T., 1995, An improved method for determining and characterizing alignments of pointlike features and its implications for the Pinacate volcanic field, Sonora, Mexico: Journal of Geophysical Research, v. 100, p. 17,659–17,670, doi:10.1029/95JB01058.

Wood, C.A., 1974, Reconnaissance geophysics and geology of the Pinacate craters, Sonora, Mexico: Bulletin of Volcanology, v. 38, p. 149–172, doi:10.1007/BF02597808.

RESERVA DE LA BIOSFERA
EL PINACATE Y GRAN DESIERTO DE ALTAR

REGULATIONS

Welcome to El Pinacate! You are in a biosphere reserve managed by the Mexican Federal Government and the Comision Nacional de Areas Naturales Protegidas (CONANP).

The reserve's park rangers and other staff members are empowered to enforce the observance of these regulations and to protect the area. They have a radio and telephone link with the Federal Plice, the Mexican Army, PROFEPA (the Environmental Protection Attorney General's Office) and the Attorney General's Office to prosecute immediately any violation of the law.

Help us preserve this area and avoid legal action be taken against you. Penalties can go from a verbal warning to incarceration.

GENERAL REGULATIONS:

- All visitors shall fill out registration form F-01 at the Visitor's Center and pay the corresponding fee (Federal Rights Law, article 198-A) or, if not possible in the field and hand it to any staff member.
- The reserve is open to all citizens' nevertheless, any visitor that might seem to be a potential danger for the reserve's or other visitor's integrity or even to himself will not be allowed to enter, such as people under the influence of intoxicating beverages or drugs.
- Weapons are strictly prohibited.
- Remains or any other type of the area's natural or cultural resources is totally prohibited.
- The use of plants or animals for feeding, heating or ritual purposes is not allowed but in some exceptional cases and only with the reserve's authorized personnel's written approval.
- It is strictly forbidden to let free domestic or exotic wild animals or to plan native or exotic plants.
- A special permit issued by the SEMARNAT and a payment receipt are required for commercial filming.
- Campfires are not allowed; portable gas, alcohol or other fuel stoves are permitted only in designated campgrounds or in the backcountry when there is no risk of starting a fire and when not done in commonly used parking areas or roads..
- We strongly recommend that you do not bring in your pets. A pet shall be let in provided it remains in your vehicle or if you keep it under control on a leash when you walk it out. In any case a permit might be denied by the staff in duty when it be considered that your pet poses a risk for the area or for other visitors.
- Very big or heavy vehicles shall not be allowed to enter, such as RVs or many-wheeled vehicles. ATV's (All Terrain Vehicles) or ORVs (Off Terrain Vehicles) and sand boogies are strictly forbidden.
- Vehicles transporting toxic, flammable, or hazardous materials shall not be allowed to enter; not even when they are in transit to other destinations.
- You shall respect and observe indications of the signaling systems that you will find within the reserve, such: NOT trespassing closed roads, NOT off-driving from authorized roads, NOT speeding (25 miles maximum speed), etc.
- Climbing down craters is not allowed.
- Loud volume audio equipment is not permitted, that is, if the sound is audible at 250 yards.
- All alcoholic beverages are strictly forbidden but those of low alcohol content such as beer and only in small amounts. The staff in duty will check up each particular case. Likewise, introduction of any substance that might be used as intoxicant or narcotic is illegal.
- Any activity that maybe a possible source of air, water, or soil pollution is forbidden, such as fluid or solid waste disposal, burning or combustion of any kind of materials, etc.
- The trash that you bring or generate during your stay shall be picked up and taken away from the reserve. Do not bury it even if it is organic garbage.
- If you defecate outdoors you shall bury your feces in a cat hole of some 8-10 inches deep; DO NOT bury toilet paper or sanitary pads in it, but put them into a plastic bag and take the bag away with you.

RESERVA DE LA BIOSFERA
EL PINACATE Y GRAN DESIERTO DE ALTAR

CAMPGROUND REGULATIONS

- If you want to camp in the reserve it is mandatory that you apply in writing for a permit (Form F-01). Hand in your application form to personnel in duty at the Visitor's Center.
- Camping shall be allowed only within predetermined sites intended for that purpose and designated by the reserve's personnel. People allocation in campgrounds will be done based on sited carrying capacity.

Authorized campsites are as follows:

∞ RED CONE

Capacity for 20 persons and /or 5 vehicles. Located at 16.2 miles northeast of the Visitor's Center. Access through a rocky and bad shaped dirt road. We recommend that you take a high vehicle. Four wheel drive is not necessary. This site doesn't have any kind of services or facilities but a few picnic tables and benches. It is the closest spot to the Santa Clara volcano (Pinacate) by road.

∞ EL TECOLOTE

Capacity for 40 persons and/or 10 vehicles. Located at 20.6 miles north of the Visitor's Center through a moderately well-shaped dirt road, somehow sandy in parts (sand and vocanic ash). It is okay for regular vehicles to transit. It doesn't have any services or facilities but a few picnic tables and benches. It is the nearest campground to the El Elegante crater (approximately 5 miles Northeast).

∞ BACKCOUNTRY CAMPING

All sites have a maximum capacity for 3 persons and no vehicles. These are located anywhere within the public area (see map) at one third of a mile away from roads, water reservoirs, craters, lava flows, lapilli areas, or archaeological sites. Access only on foot.

- We do note make camping reservations. You must register for a permit available on a first-come, first-served basis at the Visitor's Center information desk.
- If a specific campground has some vacancies it will still receive individuals or other group members that will share the place with you until the site is full to its capacity. We do not have exclusive sites.
- Pets are not allowed at either of the two established campgrounds.
- Only campfires are permitted using charcoal and fuel pellets.
- You are allowed to cook or heat your meals on portable grills or stoves within campgrounds or other campsites, provided that no risk of catching fire is present, and when not done in commonly visited parking areas or roads.
- DO NOT use rocks to anchor tents or canvas on the ground.
- Audio equipment is not allowed unless you listen to it through a headset or at low volume and provided other people are in agreement. The same applies to musical instruments such as guitars.
- **It is strictly forbidden to slide downhill for recreational purposes on volcanic-ash-covered hills, as well as to do any other destructive activity that may cause a negative impact on the soil, vegetation, fauna or archaeological remains.**

Information Center phone number (from US) 011-52-638-384-9007
E-Mail pinacate@conanp.gob.mx

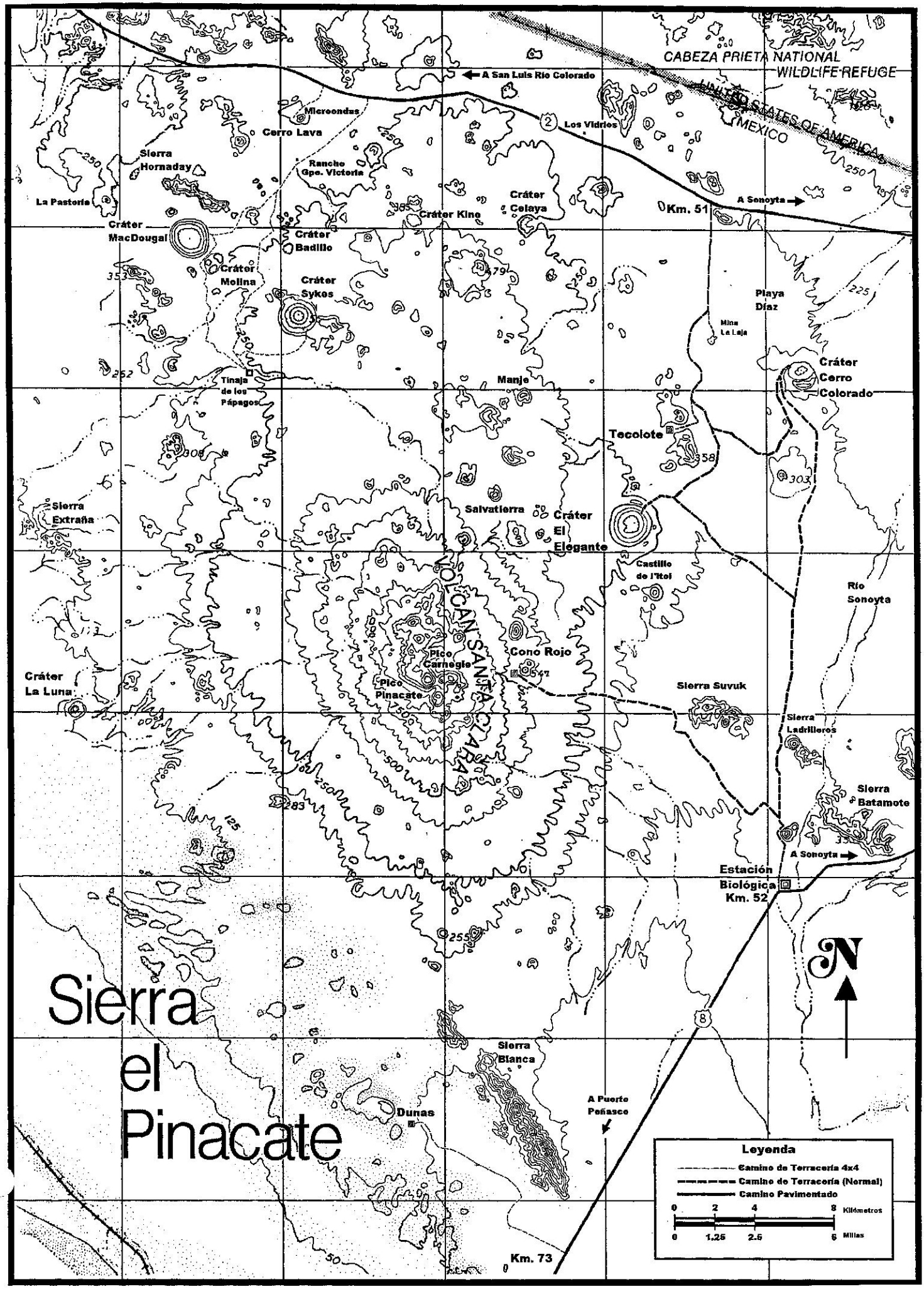
CABEZA PRIETA NATIONAL WILDLIFE REFUGE
UNITED STATES OF AMERICA
MEXICO
A San Luis Rio Colorado
Los Vidrios
Microondas
Cerro Lava
Sierra Hornaday
Rancho Gpo. Victoria
La Pastoria
Cráter MacDougal
Cráter Badillo
Cráter Molina
Cráter Sykes
Cráter King
Cráter Celaya
Km. 51
A Sonoyta
Playa Díaz
Mina La Laja
Cráter Cerro Colorado
Tinaja de los Pápagos
Manje
Tecolote
Sierra Extraña
Salvatierra
Cráter El Elegante
Castillo de l'Itol
Río Sonoyta
VOLCAN SANTA CLARA
Pico Carnegie
Pico Pinacate
Cono Rojo
Cráter La Luna
Sierra Suvuk
Sierra Ladrilleros
Sierra Batamote
A Sonoyta
Estación Biológica Km. 52
N
Sierra Blanca
Dunas
A Puerto Peñasco
Km. 73
Sierra el Pinacate
Leyenda
Camino de Terracería 4x4
Camino de Terracería (Normal)
Camino Pavimentado
0 2 4 8 Kilómetros
0 1.25 2.5 5 Millas

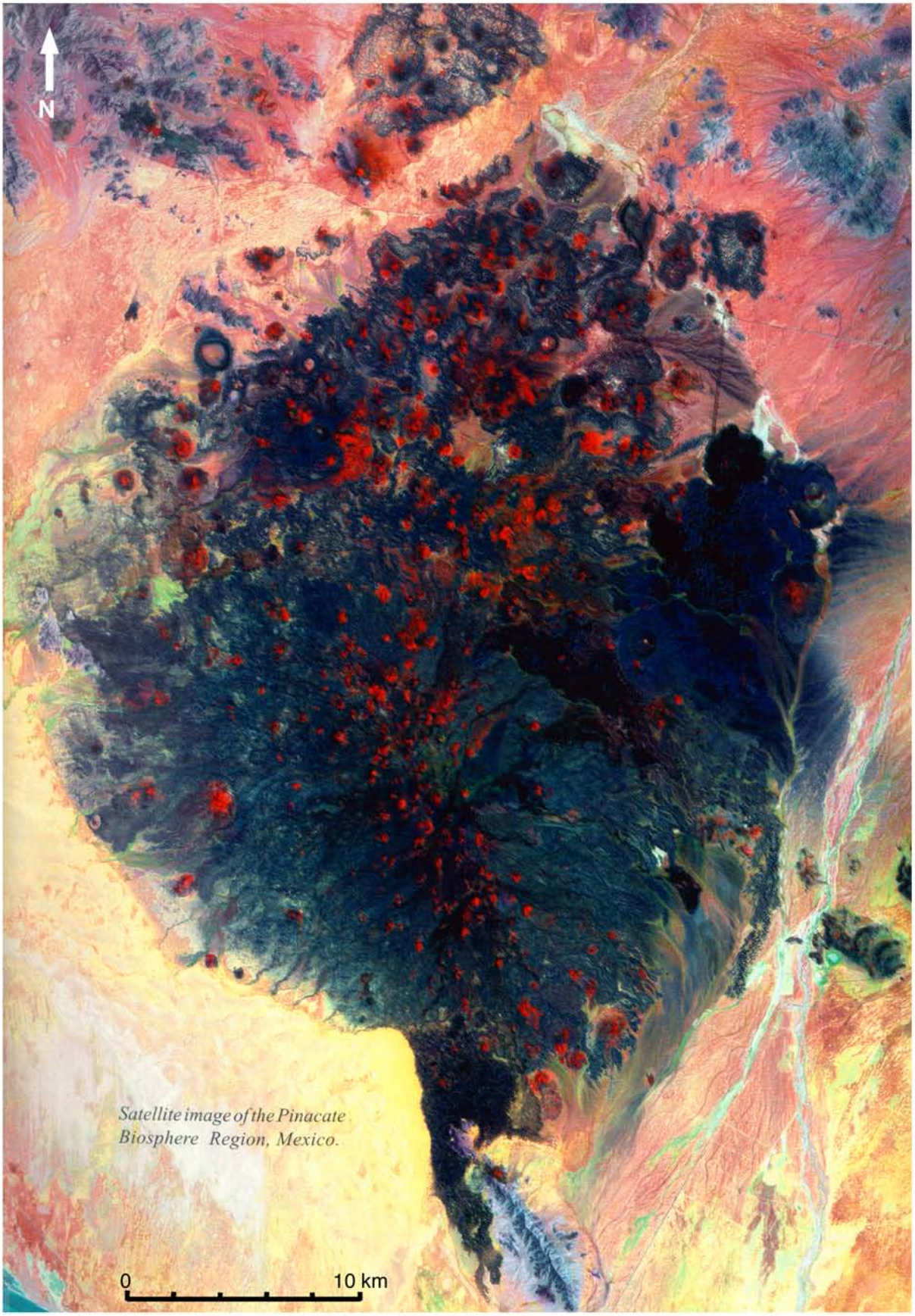

Figure 1. Landsat Thematic Mapper false color image of the Pincate Volcanic Field. Band 7 (2.08-2.35 μm) is displayed in the red channel, band 4 (0.76-0.90 μm) in green, and band 2 (0.52-0.60 μm) in blue.

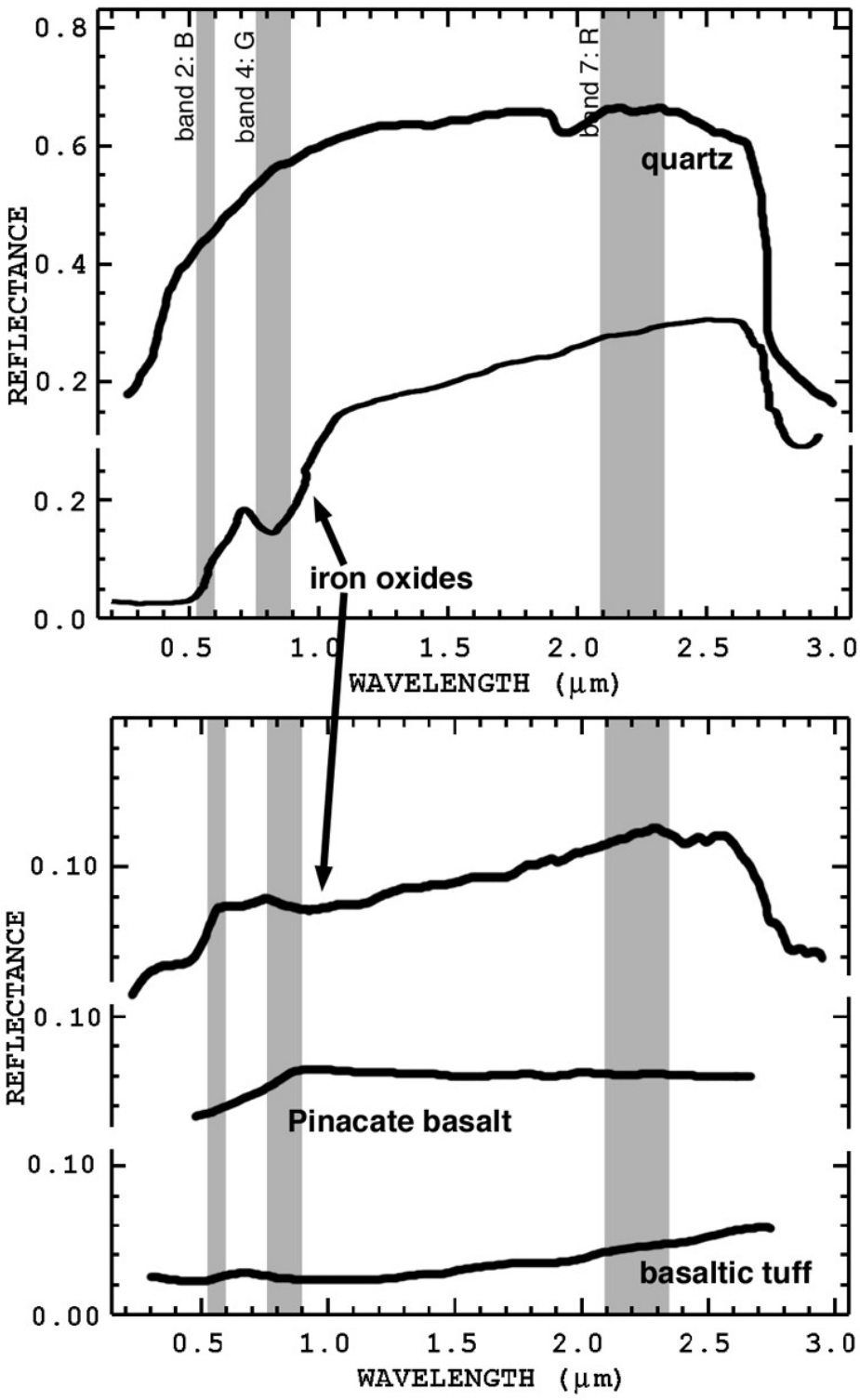

Figure 2. Reflectance spectra for rocks and minerals relevant to the Pinacate study area. Vertical bars indicate wavebands of Landsat TM data used to create false color image (Fig. 1).

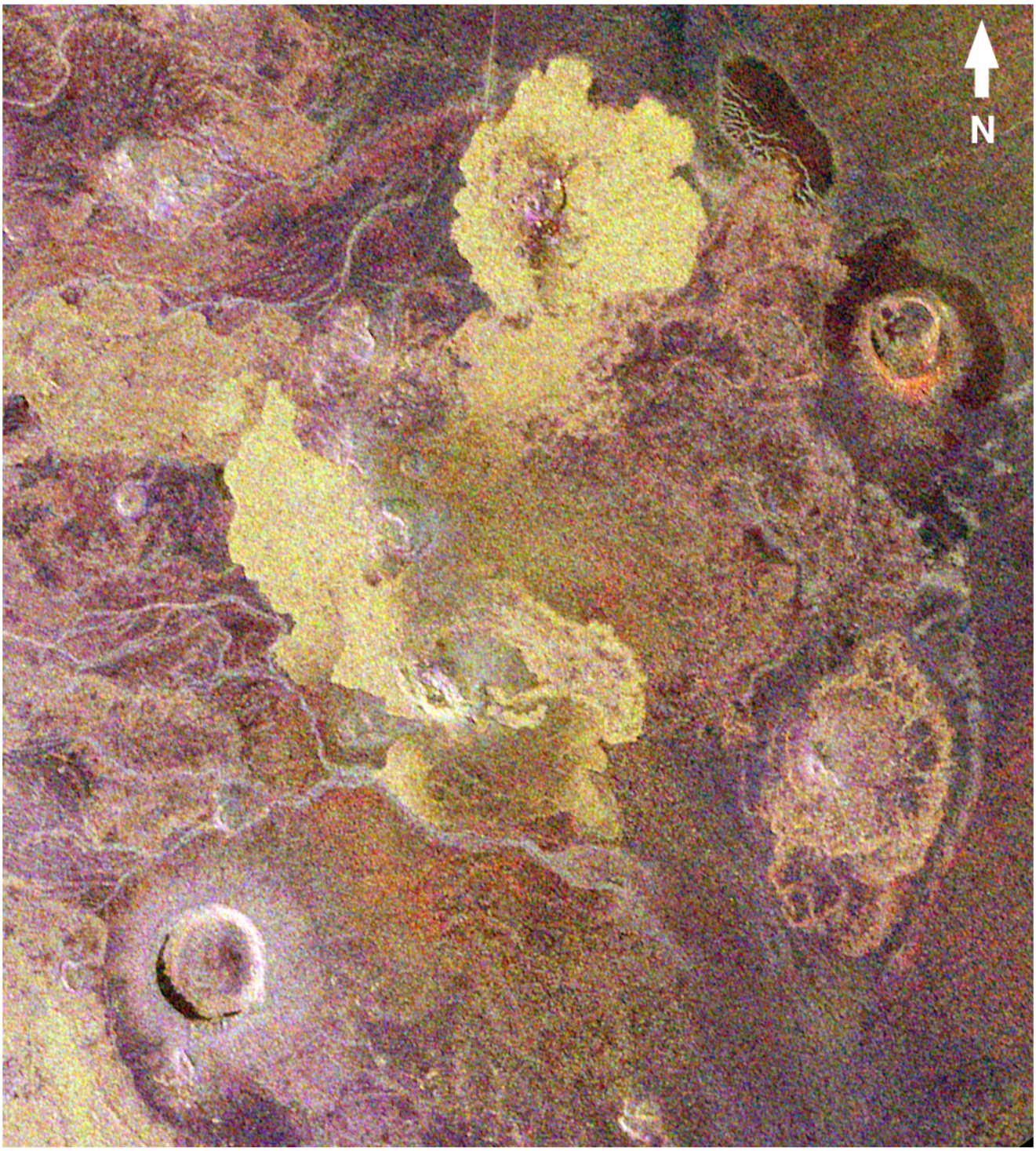

Figure 3. Enlargement of SIR-C/X-SAR image.

Airphoto of Pinacate Volcanic Field, showing Crater Elegante (E), Tecolote (T) and Mayo (M) cones

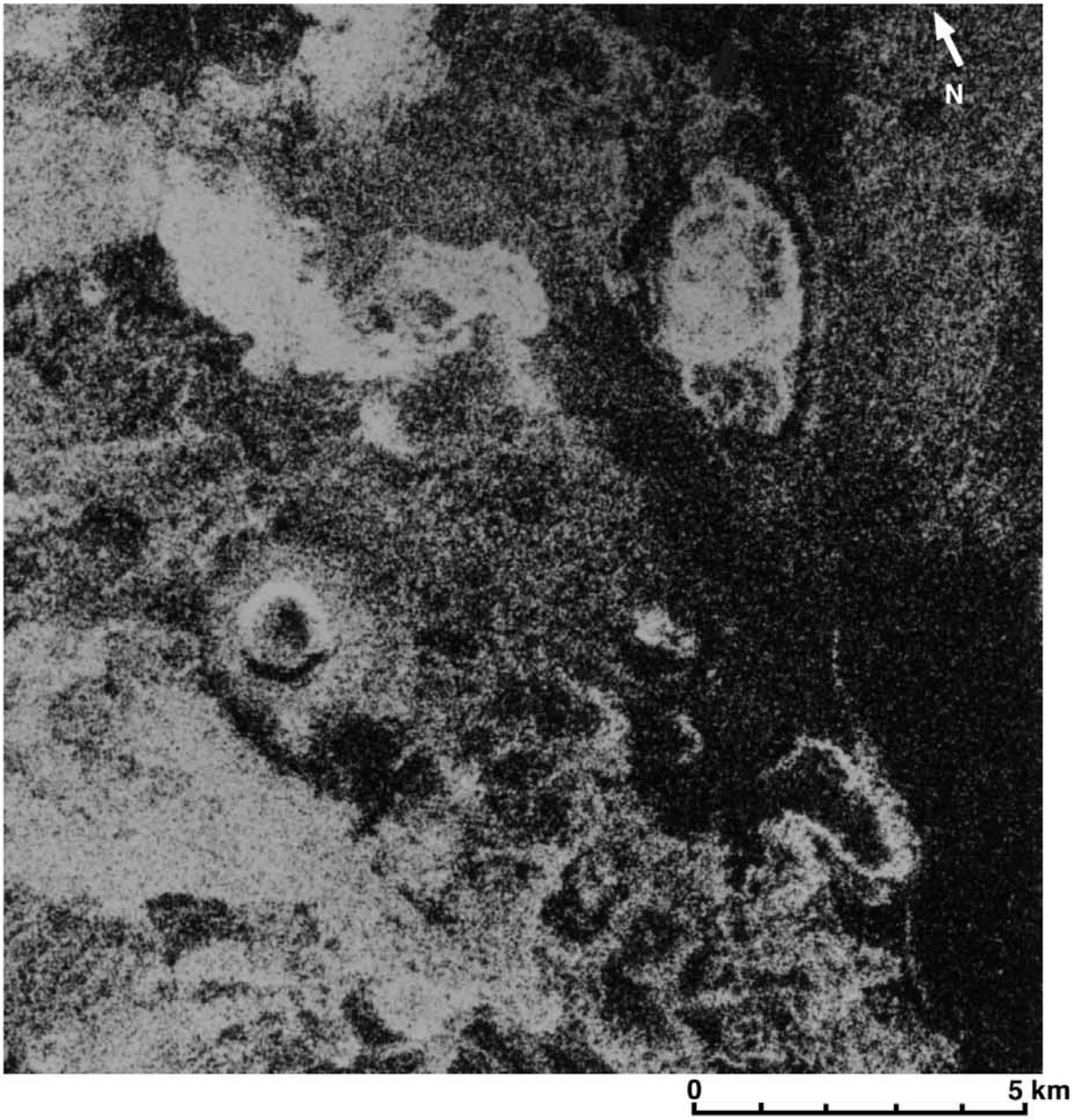

SIR-A radar image of the Pinacate Volcanic Field, showing Crater Elegante, and Tecolote and Mayo cones

GEOLOGY OF THE PINACATE VOLCANIC FIELD

by
James T. Gutmann
Department of Earth & Environmental Sciences
Wesleyan University, Middletown, Conn.
and
Michael F. Sheridan
Department of Geology
Arizona State University,
Tempe, Arizona

This 2½ day trip will cross the international border into Mexico to examine basaltic rocks in the northeastern part of the Pinacate field, including cinder cones, a large collapse depression, and a tuff cone. Participants should bring proof of U. S. citizenship, sleeping bags, ponchos, canteens, and sturdy boots. We will camp out in the Sonoran desert for two nights. The trip is moderately strenuous owing to locally precipitous terrain.

INTRODUCTION

The Pinacate volcanic field is located in northwestern Sonora, Mexico, near the northern end of the Gulf of California. The field comprises 2,000 km^2 of basaltic volcanic rocks. It is dominated topographically by the Sierra Pinacate, a broad, composite volcanic pile in the southern half of the field with a maximum elevation of 1,206 m. Many of these volcanic rocks evidently are of late Pleistocene age, although others are deeply dissected by erosion and may be considerably older. The field is characterized by an abundance of cinder cones. Many of the flows can be traced sourceward to a vent complex marked by a cinder cone and recording a multi-stage eruptive history involving alternating effusive and pyroclastic activity. In addition, the field contains eight circular collapse depressions and a partially collapsed tuff cone (Cerro Colorado). The collapse depressions, which range up to 1.7 km in diameter, are flat floored and have steep walls exposing various sequences of flows, shallow intrusions, and pyroclastic rocks. Many of these rocks represent volcanic units pierced by the crater but otherwise unrelated to it, whereas others were derived from vents located within the area now occupied by the crater and some clearly are part of the sequence of eruptions which culminated in collapse and crater formation. All of the collapse depressions are surrounded by units of tuff breccia which form crater rim deposits. These pyroclastic rocks are rich in vesicular, juvenile lapilli and ash. Some contain abundant accidental ejecta derived from unconsolidated sediment beneath the volcanic section. All contain accessory blocks and smaller fragments of holocrystalline basaltic rocks torn from vent walls during culminating phreatomagmatic eruptions.

Primary depositional structures and textures of pyroclastic-surge deposits are well displayed at Crater Elegante and Cerro Colorado. The three principal bed forms (sandwave, massive, and planar of Sheridan and Updike, 1975) show a concentric distribution consistent with the deflation model of emplacement described by Wohletz and Sheridan (in press). These features contrast with the avalanche-type bedding typical of cinder cones.

Cerro Colorado and six of the eight collapse depressions are disposed along an arcuate path trending westward across the northern part of the volcanic field (fig. 1). Ives (1936) suggested that, prior to diversion by the lavas, the Sonoita River flowed westward across what is now the northern part of the field and discharged into the Gulf of California at Pozo Caballo on Adair Bay. Jahns (1959) noted the general correspondence between the arc of collapse depressions and the ancient course of the Sonoita River and suggested that the availability of groundwater was an important element in the genesis of the tuff-breccia-forming eruptions. In providing the first general geologic description of the large, flat-floored depressions, Jahns (1959) pointed out that the volumes of accessory ejecta in their associated tuff-breccia units are much smaller than the volumes of the depressions themselves and emphasized the importance of collapse in their formation.

The majority of Pinacate lavas are relatively mafic hawaiites with about 48 wt percent SiO_2, 17 wt percent Al_2O_3, 2.7 wt percent TiO_2, 5 wt percent MgO, 12 wt percent total iron (as Fe_2O_3), 9 wt percent CaO, 4 wt percent Na_2O, and 1.3 wt percent K_2O. Small amounts of normative nepheline are indicated in a few analyses. The normative plagioclase generally is andesine although some of the lavas contain normative labradorite and are alkali

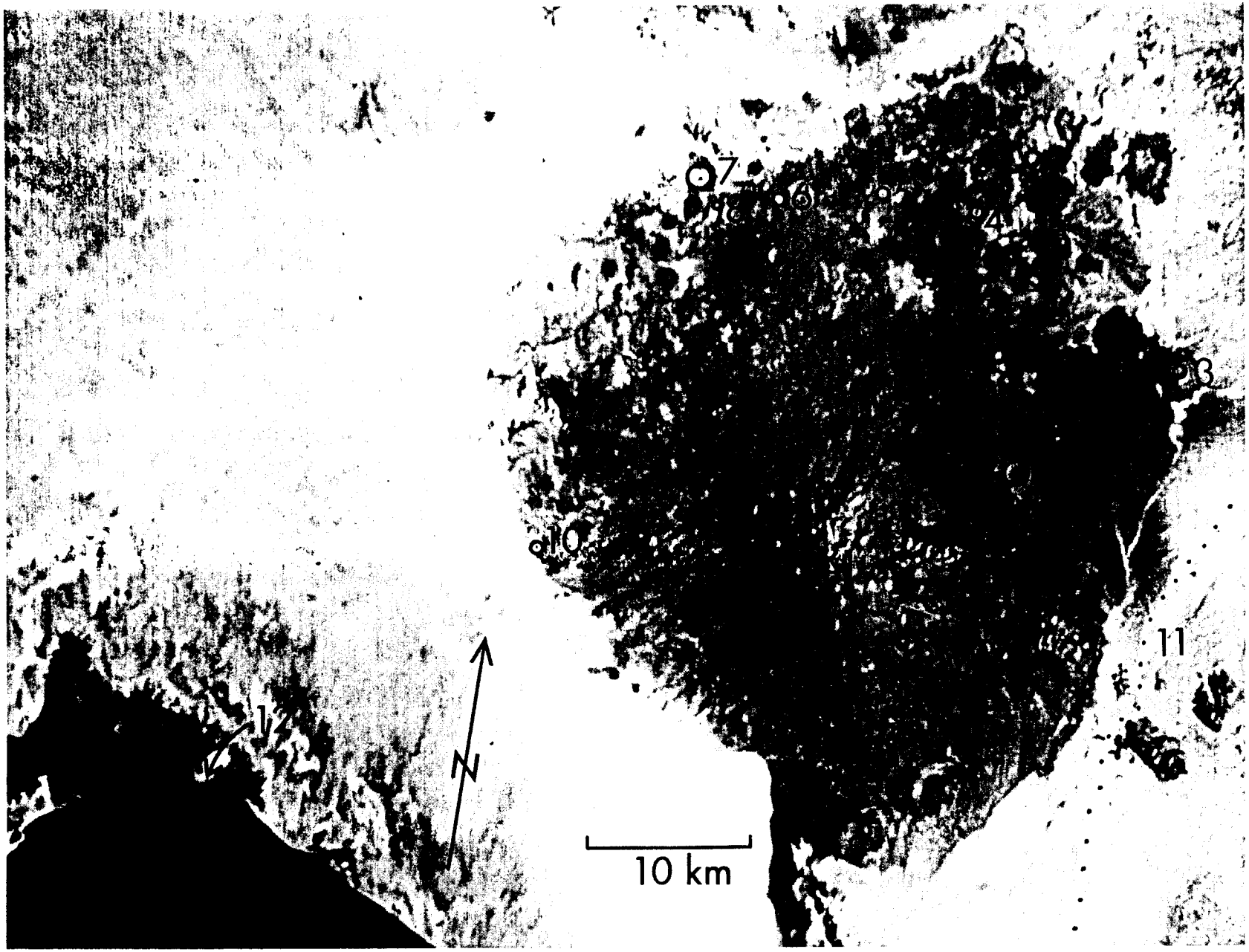

Figure 1. Pinacate volcanic field. This is a portion of a NASA photograph taken from Apollo 6. 1, summit of Sierra Pinacate; 2, Crater Elegante; 3, Cerro Colorado; 4, Celaya Crater; 5, Kino Crater; 6, Badillo Crater; 7, MacDougal Crater; 8, Molina Crater; 9, Crater Grande (Sykes Crater); 10, Moon Crater; 11, present course of Sonoita River; 12, Adair Bay on Gulf of California.

basalts. The rocks are typified petrographically by unusually large crystals of labradorite, olivine, augite, and magnetite. The labradorite crystals are as much as 10 cm in maximum dimension. The crystals of all four phases can range continuously downward in size to small phenocrysts and microphenocrysts. In thin section, many of the phenocrysts exhibit skeletal morphologies typical of rapid growth, including individuals as much as 1 cm long. Many other coarse crystals evidently have been resorbed.

Published studies in the Pinacate field include Jahns' (1959) description of the collapse depressions and Ives' (1964) summary paper on geographic aspects of the Pinacate region. The volcanic field was mapped at a scale of 1:62,500 by Donnelly (1974). Gutmann (1974) described tubular fluid inclusion textures in the coarse labradorite crystals and Gutmann and Martin (1976) described the crystal chemistry, unit cell parameters, and Al-Si ordering of these materials. Arvidson and Mutch (1974) discussed sedimentary patterns in and around five of the collapse depressions and Bull (1974) described playa processes within two of them. Wood (1974) reported the results of geophysical surveys across four of them and Gutmann (1976) described the geology of Crater Elegante. Gutmann (1977) discussed the textures and genesis of the phenocrysts and megacrysts in Pinacate lavas. Gutmann (in prep.) describes the cyclic eruptive behavior at Pinacate cinder cones and discusses controls of their activity. Wohletz and Sheridan (in press) develop a model for emplacement of pyroclastic-surge deposits using as an example the tuff breccia at Crater Elegante.

REFERENCES CITED

Arvidson, R. E., and Mutch, T. A., 1974, Sedimentary patterns in and around craters from the Pinacate volcanic field, Sonora, Mexico: some comparisons with Mars: Geol. Soc. America Bull., v. 85, p. 99–104.

Bull, W. B., 1974, Playa processes in the volcanic craters of the Sierra Pinacate, Sonora, Mexico: Zeit. F. Geomorph., Suppl. v. 20, p. 117–129.

Donnelly, M. F., 1974, Geology of the Sierra del Pinacate volcanic field, northern Sonora, Mexico, and southern Arizona, U.S.A. (Ph.D. dissert.): Stanford, Calif., Stanford Univ., 722 p.

Gutmann, J. T., 1974, Tubular voids within labradorite phenocrysts from Sonora, Mexico: Am. Mineralogist, v. 59, p. 666–672.

———1976, Geology of Crater Elegante, Sonora, Mexico: Geol. Soc. America Bull., v. 87, p. 1718–1729.

———1977, Textures and genesis of phenocrysts and megacrysts in basaltic lavas from the Pinacate volcanic field: Am. Jour. Sci., v. 277, 29 p.

Gutmann, J. T., and Martin, R. F., 1976, Crystal chemistry, unit cell dimensions, and structural state of labradorite megacrysts from Sonora, Mexico: Schweiz. Mineral. Petrogr. Mitt., v. 56, p. 55–64.

Ives, R. L., 1936, Desert floods in the Sonoyta valley: Am. Jour. Sci., v. 232, p. 349–360.

———1964, The Pinacate region, Sonora, Mexico: Occ. Papers Calif. Acad. Sci., no. 47, 43 p.

Jahns, R. H., 1959, Collapse depressions of the Pinacate volcanic field, Sonora, Mexico: Ariz. Geol. Soc., Southern Arizona Guidebook 2, p. 165–184.

Shakel, D. W., and Harris, K. M., 1972, Potsherd evidence for minimum age of Cerro Colorado crater, Pinacate volcanic field, northwestern Sonora, Mexico: Geol. Soc. America, Abs. with Programs for 1972, v. 4, p. 408.

Sheridan, M. F., and Updike, R. G., 1975, Sugarloaf Mountain tephra—A Pleistocene rhyolite deposit of base-surge origin in northern Arizona: Geol. Soc. America Bull., v. 86, p. 571–581.

Wohletz, K. H., and Sheridan, M. F., in press, A model of pyroclastic surge: Geol. Soc. America Memoir.

Wood, C. A., 1974, Reconnaissance geophysics and geology of the Pinacate craters, Sonora, Mexico: Bull. Volcanol., v. 38, p. 149–172.

ROAD LOG AND STOP GUIDE

MILES Interval	Total	
		1st DAY (Leave Tempe, Ariz., at noon).
0.0	0.0	Corner of Rural Road and Apache Boulevard, Tempe. Head south on Rural Road to the Superstition Freeway on-ramp. Take the Superstition Freeway west to Interstate 10.
4.9	4.9	Junction Interstate 10. Take Interstate 10 south toward Tucson.
8.0	12.9	Maricopa exit. Take the interstate off-ramp south to Maricopa.
16.8	29.7	Town of Maricopa.
13.0	42.7	Junction Arizona 84. Turn west toward Gila Bend.
6.1	48.8	Junction Interstate 8. Keep west toward Gila Bend.
40.4	89.2	Gila Bend. Take the Interstate 8 off-ramp for Arizona 85 south toward Ajo.
40.6	129.8	Ajo.
13.5	143.3	Why. Bear south on Arizona 85.
28.2	171.5	International border at Lukeville. Be prepared to obtain Mexican tourist permit to visit Parque Natural del Pinacate. Valid proof of U.S. citizenship is needed (birth certificate, passport, or voter registration card).
2.0	173.5	Town of Sonoita. Bear right (west) on Mexico Rte. 2 toward San Luis.
31.6	205.1	Bear left on dirt road at sign marking entrance to Parque Natural del Pinacate (a unit of the Mexican counterpart of the U.S. National Park system).
3.8	208.9	Bear right (west) on dirt road.
6.0	214.9	Road junction. Continue straight ahead (stay right).
0.4	215.3	**STOP 1.** Steep front of an aa flow. Most Pinacate flows are aa flows with extremely rough surfaces. This flow emerged from a breach in the large (150 m high), young cone to the west. It overlies ejecta from that cone;

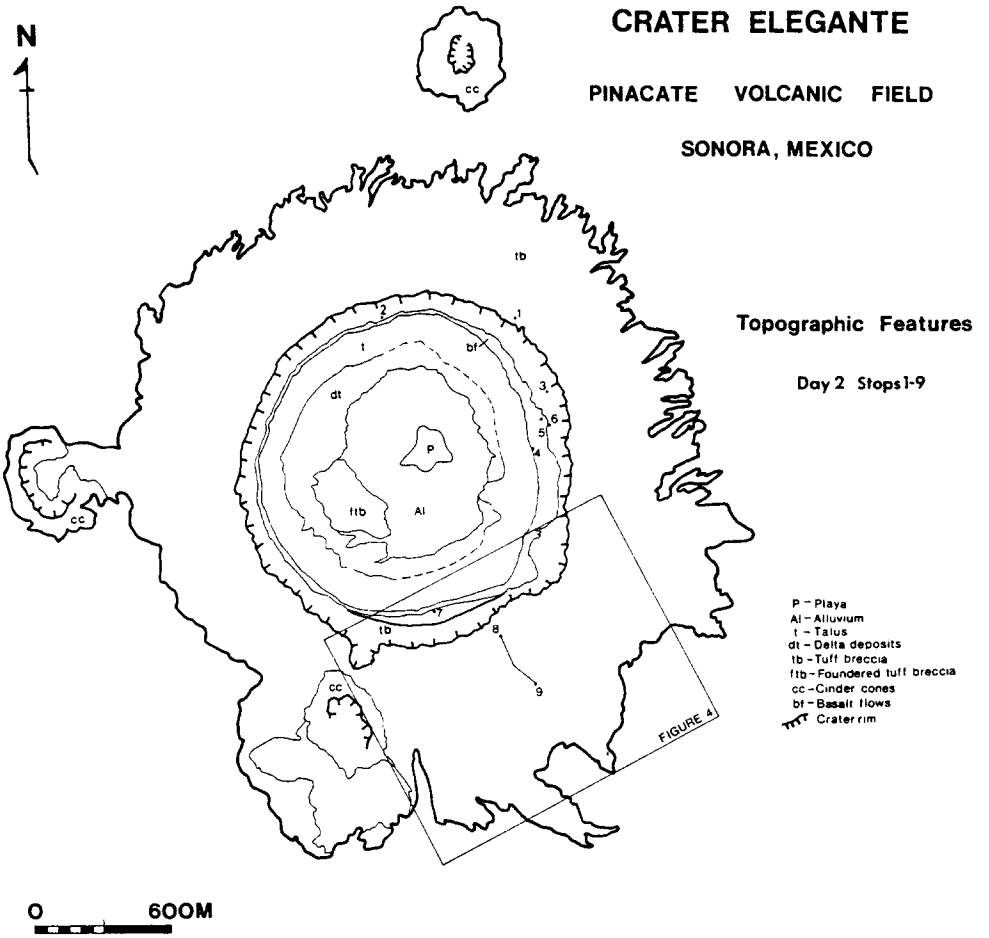

Figure 2. Sketch map of Crater Elegante. Major units indicated by key. Stops for DAY 2 given by numerals. (Modified from Gutmann, 1976.)

these ejecta also occur resting on the flow as scattered masses of cinder derived and rafted from the breach in the wall of the cone. Pale yellow, gem-quality labradorite megaphenocrysts up to 5 cm long occur sparingly in this flow and in cinders near the vent.

2.8 218.1 Road junction. Continue straight ahead.

0.9 219.0 Road junction. Camp here.

2nd DAY

Walk the road 1 km up to the rim of Crater Elegante. Figure 2 shows stops for today and a general plan view of the crater and environs.

STOP 1. Crater Elegante is 1.6 km in diameter and 244 m deep. The stratigraphic record revealed in its walls includes four major parts (see Gutmann (1976) for details). The oldest exposed rocks are flows of mafic hawaiite, many of which evidently originated at the cinder cone immediately south of the crater, both preceding and accompanying pyroclastic eruptions there. Erosional dissection of this cone prior to deposition on it of Elegante tuff breccia suggests that it is considerably older than Crater Elegante.

Resting on these old flows is a cinder cone, the vent for which lay in the southeastern part of what is now the crater. This "gray cinder" cone is displayed in cross section in the crater walls (fig. 3); it was breached to the southeast following emplacement of sills within the cone structure and along its base south of the vent. Renewed eruptions from essentially the same vent then produced cinder units ("brown cinders"), flows, and dikes, all of which are especially rich in phenocrysts.

Cinder eruptions occurred next from a vent in the southern part of what is now the crater; these were immediately preceded by a flow that baked the base of the overlying cinder section locally.

Finally, a flow was erupted from a vent probably located near or somewhat northeast of the center of the crater. Minor cinder eruptions may have followed this flow but the nature of eruptions changed quickly as groundwater gained access to the vent and magma column. The ensuing phreatomagmatic eruptions gave rise to the unit of tuff breccia that forms the crater's rim beds. This unit is as much as 70 m thick in the northeastern parts of the rim. Its chief constituents, listed in order of decreasing abundance at the rim, are vesicular pellets of glassy, juvenile ash rich in tiny crystals, accessory blocks and smaller fragments of holocrystalline basalt torn from vent walls, and quartzofeldspathic sand, silt, and clay of accidental origin.

Accessory ejecta decrease rapidly in abundance with distance from the crater rim, while the abundance of accidental ejecta increases in the same direction. An upper limit on the amount of accessory debris deposited outside the crater indicates that the diameter of the vent piercing the volcanic section was not greater than 672 m and may have been considerably less. A vent of this size implies the former existence of a tuff breccia cone over much of the site of the present crater. The large hill apparent on the crater floor consists of tuff breccia and probably represents the upper parts of this vanished cone. Crater Elegante formed chiefly by wholesale collapse when the volcanic edifice subsided into a phreatomagmatic explosion chamber developed within fine-grained sediment beneath the section of volcanic rocks.

Proceed counterclockwise around the crater rim to a point due north from the center of the crater.

Descend to the base of the rim bed section. WATCH YOUR FOOTING AT BRINK OF CLIFFS.

STOP 2. Contact of tuff breccia with underlying flow. This flow was mobile when the tuff breccia was deposited on it and flowed in response to differential loading with tuff. Flow-top breccia is largely absent here but present nearby to east and west. Note the wavelike bulge of the flow top with crest subparallel to the crater rim, the curious "sharktooth" texture of the upper surface of the flow here, the dike originating within the flow and cutting the overlying tuff, the contact effects on the tuff adjacent to this dike, and the folds and faults within the lower 10 m of the tuff breccia section. Note also scattered small xenoliths and xenocrysts of quartzofeldspathic debris in the flow. Such accidental inclusions are rare in Pinacate flows. Their presence here indicates admixture of sediment within the magma column somewhat prior to the onset of phreatomagmatic eruptions.

Return to the crater rim. Proceed clockwise around the rim to a point on bearing 63° from the center of the crater. Descend toward the base of the rim bed section.

STOP 3. The descent route traverses a well-exposed section of the tuff breccia. Note the gray unit of lapilli tuff about half way down through the section; this unit is relatively poor in ash and accidental ejecta but unusually rich in frothy juvenile lapilli, as if the supply of meteoric water and sediment temporarily diminished during the culminating eruptions. Excellent exposures of tuff breccia occur further down the slope. Note the lens of coarse breccia at the base of the section here. This breccia is rich in accessory blocks and juvenile lapilli but poor in ash; it evidently represents early, vent-clearing explosions consequent upon initial access of abundant meteoric water to the magma column.

Descend through the underlying cinder section to the edge of the cliffs. The massive buttress to the north is an intrusion petrographically related to the brown cinders and probably emplaced laterally through the cinder section from a source to the south.

Traverse left (south) about 200 m along the base of the gray cinder section to a prominent vertical dike.

STOP 4. Lowermost parts of a composite dike of porphyritic basalt cutting the gray cinders. Both the keel and the crest of this dike are exposed. Its crest is grossly horizontal and extends northward more than 100 meters to the top of the section of gray and brown cinders. There the dike fed a small flow upon which the tuff breccia was deposited. Presence of the keel and attitude of the crest indicate that the dike was emplaced horizontally through the cinder section from a source to the south near or coinciding with the vent of the gray and brown cinders.

The dike here comprises several pairs of narrow, vertical zones symmetrically disposed about its core and recording the passage and chilling of successive pulses of magma. The core of the dike is occupied by an intrusion of chilled, porphyritic basalt which widens upward in the dike. Note the increase in size and abundance of the coarse labradorite megaphenocrysts inward to a zone especially rich in these as well as in small xenoliths and pea-sized crystals of olivine. This inward increase suggests flowage differentiation. At the same time, the groundmass of the dike is depleted in plagioclase relative to that of nearly aphyric Pinacate lavas such that the entire intrusion is not significantly enriched in plagioclase. The numerous giant labradorite crystals evidently formed from the liquid whose other solid products now enclose them and are truly phenocrysts. Please refrain from sampling the dike at this locality.

Also well exposed here are the lower parts of the gray cinder section. The tan layers within this section contain quartzofeldspathic sand and silt of accidental origin together with abundant juvenile ash and lapilli. The juvenile constituents are highly vesicular glass with numerous tiny crystals and some are slightly palagonitized. These tuffaceous layers evidently represent phreatomagmatic interaction between wet sediment and briskly vesiculating magma in the conduit. Implied breaches, periodically reopened in the conduit walls during the early phases of cinder eruption, must have been sealed or failed to provide copious amounts of meteoric water, however, for ash and accidental ejecta are largely absent from the bulk of the gray cinder section.

LUNCH STOP. Some may wish to traverse south along the base of the gray cinder section toward the vent region. Descent to the talus slope rising from the floor of the crater is easy near the vent and affords access to a thick dike that fed a laterally extensive, shallow intrusion emplaced within the lowermost parts of the gray cinder pile (Devil's

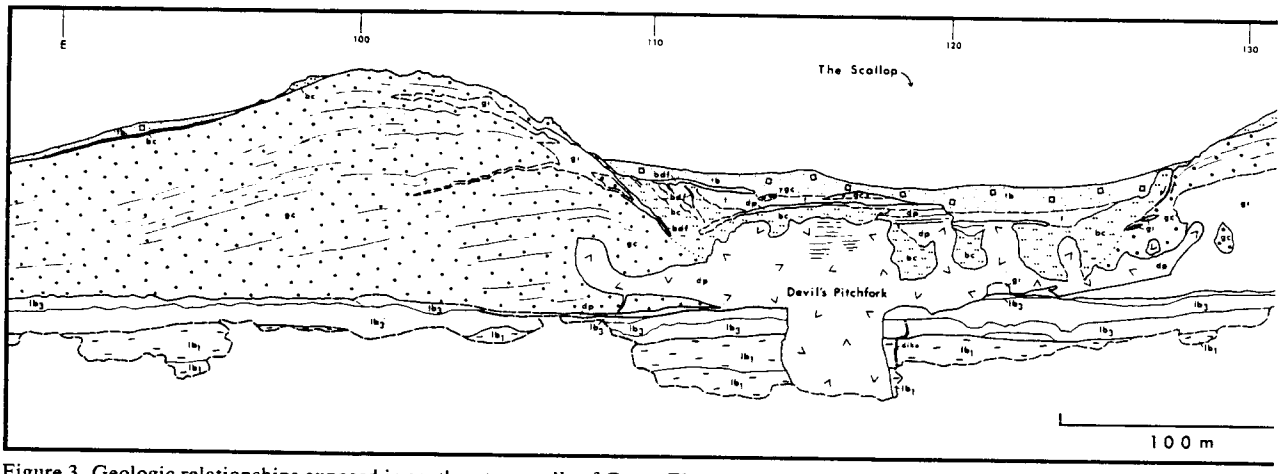

Figure 3. Geologic relationships exposed in southeastern walls of Crater Elegante as seen from the center of the crater floor. Numbers along the top of the figure give azimuths from center of crater. No vertical exaggeration. lb_1 and lb_3—lower basalt flows; gc—gray cinders; gi—gray intrusions; bc—brown cinders; bdf—dikes and flows associated with brown cinders; rdc—ribbon dike cinders; rds—ribbon dike and sill; dp—Devil's Pitchfork intrusion and associated flows; ygc—younger gray cinders; tb—tuff breccia; t—talus.

Pitchfork of fig. 3). Others may wish to traverse about 100 meters southward and descend over the flows and down over talus to the crater floor. Noteworthy features of the crater floor include the foundered mass of tuff breccia, topset and foreset deposits in a lake that formerly occupied the crater to a maximum depth of about 60 m, and large oval subsidence pits and linear depressions within the playa.

Return northward 50 m from the keel of the dike and ascend the gully to the upper parts of the dike.

STOP 5. The thin crestal parts of this dike contain sheetlike gas cavities at the core. These megavesicles are a few cm wide but can be a few meters in vertical dimension or parallel to strike of the dike. They probably represent accumulation of gas in the upper parts of the intrusion. Note the "drips" of magma on exposed walls of the gas cavities. These drips consist of porphyritic basalt that was too viscous to flow to the bottoms of the sheetlike voids.

Ascend southward to the crest of the dike. Note bifurcations of the dike.

STOP 6. The crest of the dike here lies just below the top of the gray cinder section. The overlying section of brown cinders contains scattered, subhedral to euhedral, single crystals of labradorite as much as 5 cm long. Euhedral phenocrysts of olivine and magnetite a few mm across also occur in this unit, as do augite crystals up to 3 cm in maximum dimension.

Ascend to the crater rim and proceed clockwise around the rim. The scallop-shaped depression in the southeastern rim of the crater reflects breachment of the gray cinder cone through its eastern flank as well as several subsequent events. Tumuli of the breaching flow are apparent on the flats to the east. Continue around the rim to a point on bearing 168° from the center of the crater. Descend through the tuff breccia section and younger gray cinders to the top of the highest flow.

STOP 7. Contact of younger gray cinders on a flow. The younger gray cinders attain maximum thickness in this region. The cinder layers dip gently southward and dips increase upward in the section to as much as 13° near the top. The vent evidently was located in the southern part of the area now occupied by the crater. The phenocryst assemblage in the cinders is identical to that of the underlying flow, which rests on gray and traces of brown cinders with very different phenocryst assemblages. Where flow-top breccia separates the flow from the overlying younger gray cinders, the lowermost few meters of these cinders are faintly pinkish. Where flow-top breccia is absent, as at this locality, the basal cinders are oxidized and indurated to form a resistant, red cinder ledge a few tens of cm thick. These cinders were baked by the underlying flow, which must have immediately preceded them, presumably from the same vent. This represents the third instance at Crater Elegante wherein a flow *preceded initiation* of pyroclastic eruptions.

Return to crater rim and walk eastward back along the rim to a point on bearing about 145° from the center of the crater.

STOPS 8 and 9. Outcrops of tuff breccia surrounding Elegante Crater extend slightly less than one crater diameter from the present rim, where they range from 40 to 70 m in thickness. Their dips range from nil to 2° for distal beds to about 15° outward at the crest of the rim. These beds are characteristic of pyroclastic-surge deposits, features that are becoming much more widely recognized and better understood.

Radial dissection of the rim beds provides excellent exposures of pyroclastic surge deposits south of the crater.

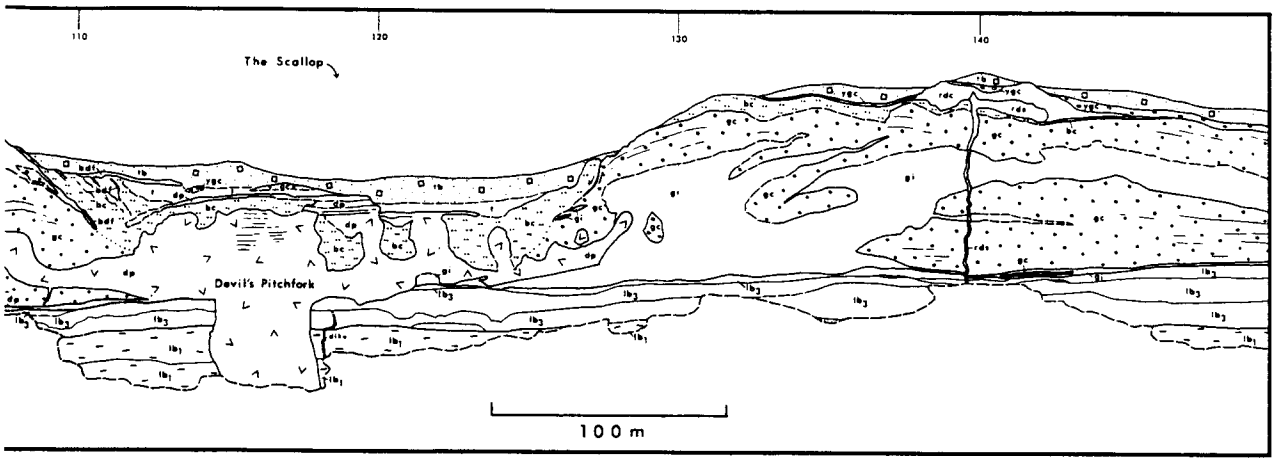

Figure 4 shows a plane table topographic map of the southern portion of the tuff deposits with the location of 30 measured sections. We will proceed down one of the south-trending gullies to observe the primary structures as well as the lateral and vertical variation of the deposits.

There are three principal bed forms in pyroclastic surge deposits (Sheridan and Updike, 1975): 1) sandwave, 2) massive, and 3) planar. Particles deposited in a sandwave bed were transported by saltation or dilute suspension in a surge blast. Massive beds were emplaced as a relatively dense suspension of particles with a bulk void fraction of 0.6 to 0.9. Planar beds represent yet more dense, only slightly dilated, traction carpets with a void fraction of less than 0.6. Complete transition occurs between bedding types, and outcrops may show one bedform that grades into another.

Three measured sections illustrate the variation of structure with distance from the rim (fig. 5). Sections 1B, 1E, and 1H are located 100 m, 225 m, and 525 m respectively from the present crater rim. The proximal section (1B) is dominated by sandwave beds, the medial section (1E) by all three bed-form types, and the distal section (1H) by planar beds. Using a Markov technique, Wohletz and Sheridan (in press) defined surge facies for every measured section. The boundaries of these three facies (sandwave, massive, and planar) are shown on figure 4. The pattern of facies distribution is similar for all pyroclastic-surge deposits studied: the sandwave facies is proximal, the massive facies medial, and the planar facies distal.

The data from three groups of spatially related, measured sections were used to reconstruct the generalized surge cloud as a function of distance from the present rim. Figure 6 shows the reconstructed cloud for Elegante surges at the southern part of the crater. This construction requires an assumption of void space during flow for each bed-form type in order to expand the measured section to flow heights. Obviously the surge clouds collapse or deflate with distance, giving rise to a deflation model of surge transport (Wohletz and Sheridan, in press).

Field and experimental evidence support the assumed flow densities. A good example of the type of exposure that allows flow density calculation is near station 5F (fig. 7). Here an accessory block in a massive bed occurs with relationship to bedding such that the bed around it must have deflated after coming to rest. The thickness of the flowing bed (h_f) was somewhat more than 31 cm and the present thickness (h_p) is 24 cm. The density of the flowing bed relative to the present bed, given by h_p/h_f, is 0.77. The void fraction (Φ) is given by the equation below:

$$\Phi = \frac{\rho_p - \rho_b}{\rho_p} = 1.0 - \frac{\rho_b}{\rho_p}$$

where ρ_p is the particle density and ρ_b is the bulk density. Assuming a particle density of 3.0 gr/cc and a rest bulk density of 1.2 gr/cc, the bulk density of the flow was 0.92 gr/cc and the void fraction (Φ) is then 0.69. Other values from outcrop data as well as experimental data from fluidized systems yield void fractions for massive beds from 0.6 to 0.9.

The planar beds are analogous to the grain dispersion flows that commonly produce inverse grading. Their void fraction of 0.6 is that which will just allow the dilation of beds so that they flow down slope. A sandwave void fraction of greater than 0.9 is taken from the results of wind tunnel experiments in which grains saltate or travel in a dilute suspension.

In making the radial traverse you should see lateral and vertical transition from sandwave to massive and from massive to planar types. Planar to sandwave or sandwave to planar transitions are rare.

Other structures also occur here. Because the massive beds are deposited in a near-fluidized, inflated condition,

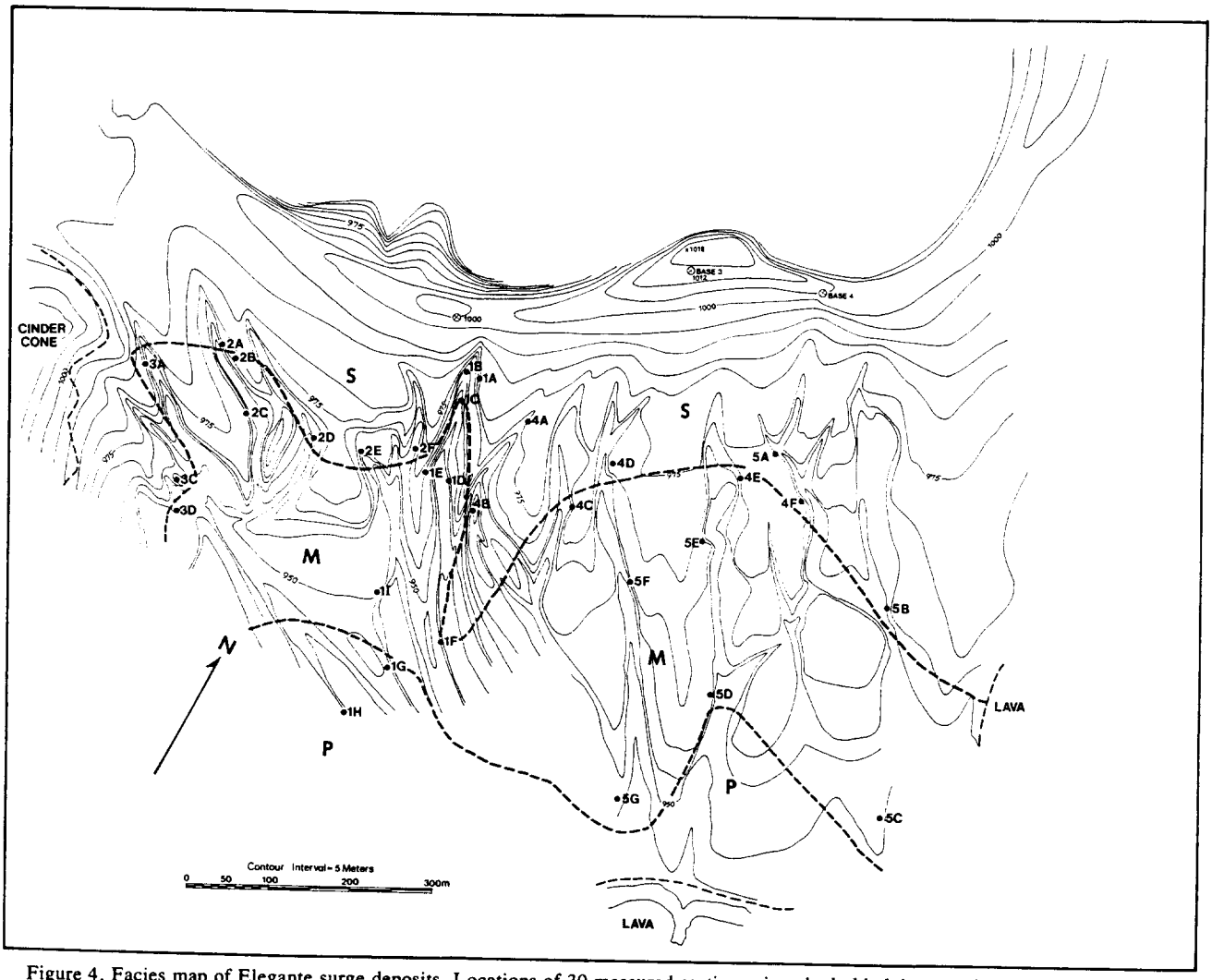

Figure 4. Facies map of Elegante surge deposits. Locations of 30 measured sections given by bold alphanumeric characters. Sandwave (S), Massive (M), and Planar (P) facies indicated by bold capital letters. Contours give relative elevation. Location of this figure given in Fig. 2.

they show many soft-sediment types of structural features, such as slump and flame structures, and bedding sags due to ballistic impact of blocks.

3rd DAY

MILES Interval	Total	
		Return eastward, retracing route of 1st day.
0.9	0.9	Road junction. Continue straight ahead.
3.0	3.9	Road junction. Continue straight ahead (stay left).
6.0	9.9	Junction with major road connecting Rte. 2 with quarry at cinder cone. Bear right (south).
0.2	10.1	Gate (normally locked) at entrance to quarry workings in young cinder cone. Cinders are mined here for construction and decorative purposes. Drive through the gate and around to the quarry.

STOP 1. This is one of the youngest cones in the Pinacate field. An unusual and particularly noteworthy feature of the eruptive history of Pinacate cinder cones is the eruption of flows from the vent *prior to* building of the cone. Although it cannot be demonstrated at this locality, exposures of the volcanic stratigraphy in the steep walls of several of the collapse depressions show that lava flows were the initial eruptive products at many Pinacate cinder cone vents. Exposures at this particular locality provide evidence that cinder eruptions ensued while the basal flow still was both hot and mobile. This flow, mantled with cinder, is exposed south of the cone. The lapilli are welded to the top of the flow locally and the lowermost parts of the cinder section are reddened and oxidized where they rest on the basal flow.

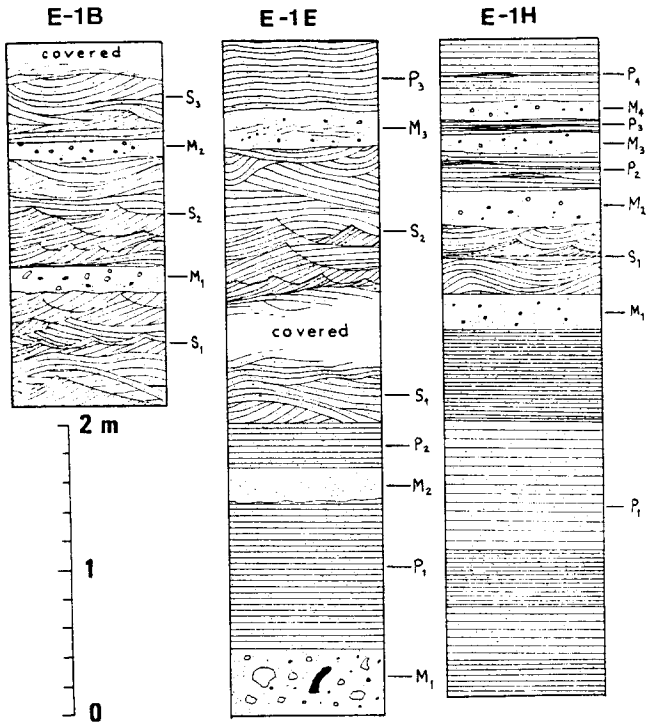

Figure 5. Measured sections of typical sandwave (E–1B), massive (E–1E) and planar facies (E–1H). Section locations shown in Fig. 4.

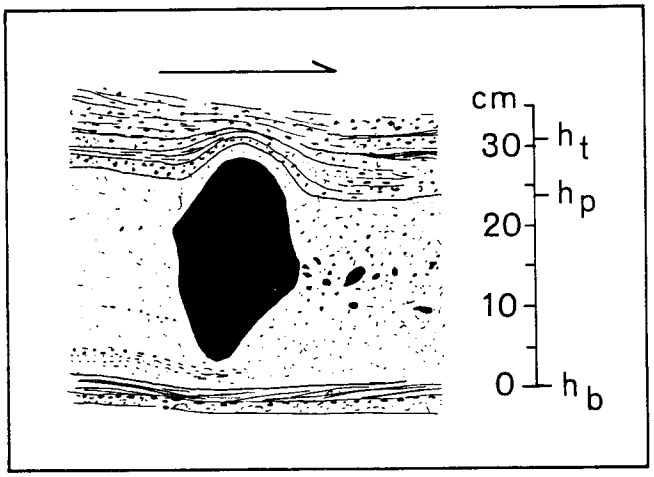

Figure 7. Compaction of massive bed due to degassing. The void fraction during flow for this bed is 0.77.

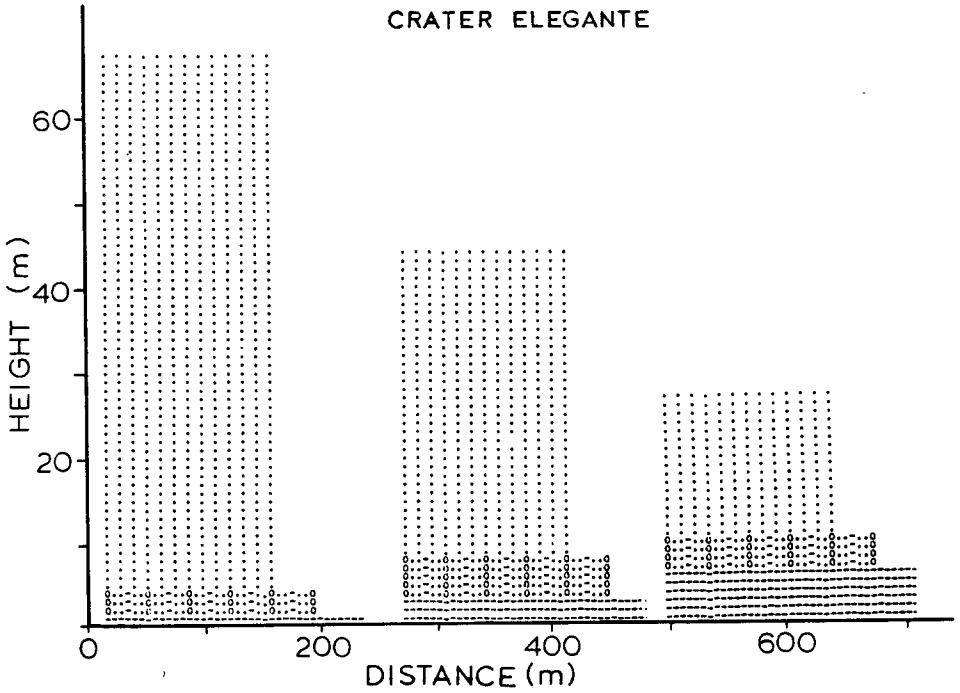

Figure 6. Deflation model of cumulative Elegante surge cloud. Data compiled from sections averaged over intervals of 0–300 m, 300–600 m and greater than 600 m. Cloud height calculated from assumed voidage ratios of 0.95 for sandwave beds, 0.75 for massive beds and 0.60 for planar beds. Distance measured from present rim. From Wohletz and Sheridan (in press).

The exposed parts of a small, dome-like hummock a few meters high immediately south of the cone comprise oxidized and indurated lapilli, probably very near the base of the cinder section, which were baked by the underlying flow. Dips of the cindery layers in the sides of this anticlinal hillock attain at least 65° and reflect folding of the cinders during development of a tumulus on the moving flow beneath. Exposures in the walls of the cinder quarry in April, 1976, revealed that normal faults cut the layering of at least 12 m of the lower parts of the cinder section in the flank of the cone (fig. 8). The strike of these faults appeared roughly perpendicular to the flow direction of the underlying basal flow and the faults dipped steeply away from the vent region. Thus, the side away from the vent was the downthrown side. The throw of the faults was as much as 1 m. These structural features indicate that the flow still was mobile after a substantial portion of the pyroclastic section had been deposited upon it. Continued motion of the basal flow away from the vent probably reflects differential loading of the molten layer by the cinder pile. Mobility of the flow is reasonable in light of the rapidity with which cinder cones can be built and the efficacy of insulation of the flow by the overlying cinders.

The summit of this small cone, which is about 80 m high, affords a good view of the tuff cone of Cerro Colorado to the east-southeast and of the northeastern marginal parts of the volcanic field. The cinder cone is breached to the north. A breaching flow, which moved southward around the cone, rafted numerous, very large masses of cinder from the breach. Nearly all Pinacate cinder

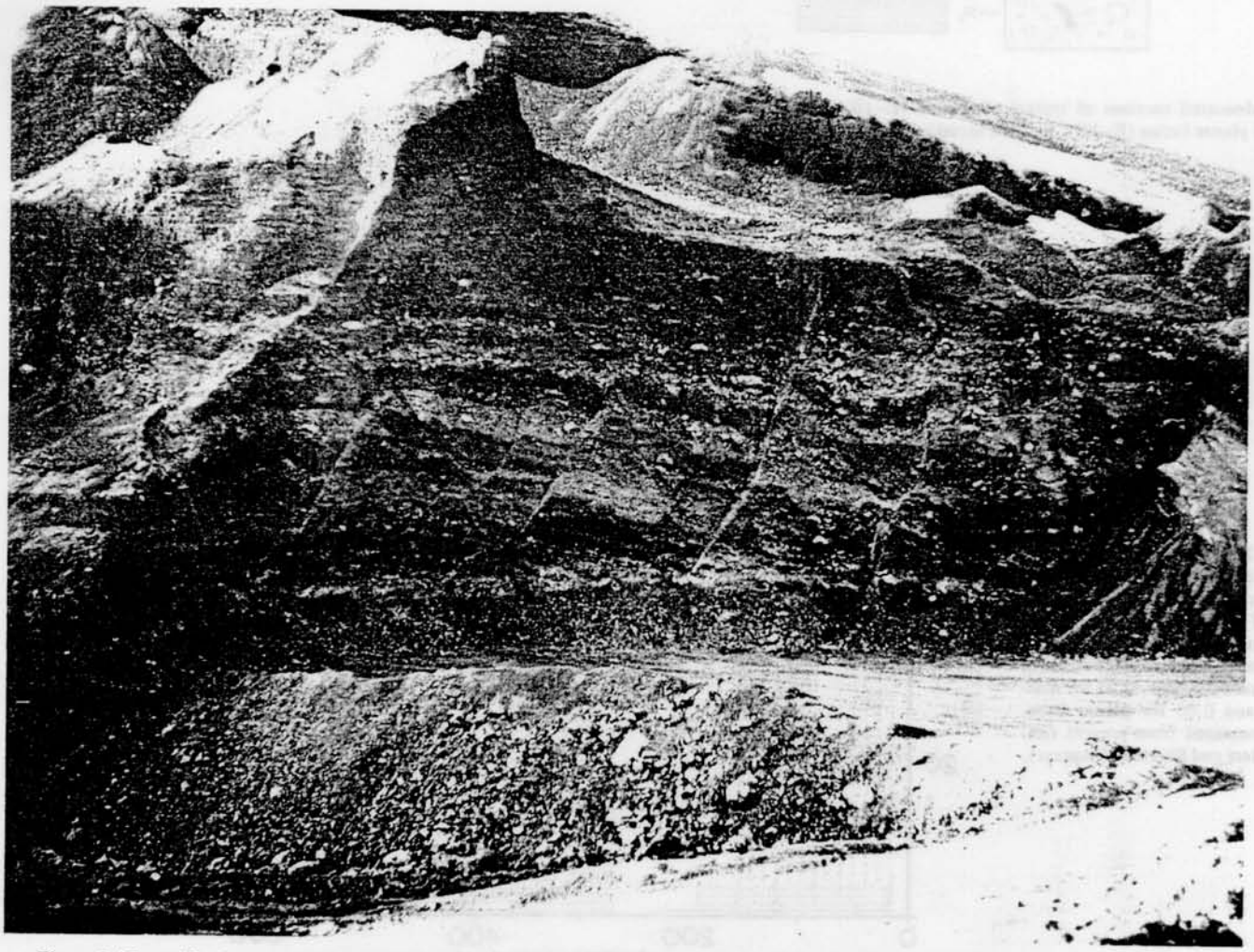

Figure 8. Normal faults cutting lower parts of the cinder section in the flank of the cone at STOP 1, 3rd day. The level crest of the vertical wall of the quarry here is about 9 m above the adjacent quarry floor.

cones are breached in similar fashion. At several localities, vertical dikes extending radially outward from the vent cut the lower half to three quarters of the cinder section and suggest that magma welled up to high elevations within the cinder cone structure prior to breachment. Abrupt truncation of the cinder layers in the walls of the breach commonly indicates removal of rafted masses of cinder when the wall of the cone finally failed owing to outward pressure from the contained lava lake. At some localities, cinder layers wrap down into the breach, as if this opening was maintained by continued or periodic flowage from the vent during pyroclastic eruptions. However, in many instances upwelling of magma occurred following the close of pyroclastic eruptions which had built an unbreached cone. Breachment may have attended development of fluid pressure in the contained lava lake sufficient to lift the surrounding cinder walls and give rise to sills at the base of the cone structure.

Return to cars. Cars return to gate. Resume road log mileage at gate.

0.2	10.3	Bear right (east) on dirt road.
3.1	13.4	Road junction. Bear right (south).
0.3	13.7	Road junction. Fork left.
0.4	14.1	Cerro Colorado. Park cars and walk east to the highest point on the north rim of the crater for lunch.

STOP 2. The crater of Cerro Colorado is about 1,000 m in mean diameter and its floor is more than 110 m below the highest point on the rim of the tuff cone. In the western wall of the crater, the tuff rests on a flow from an unknown source to the west; at the foot of the northern and eastern walls, exposures of the basal contact show that the tuff rests here on pinkish tan mudstone that probably represents playa deposits. The eruptive history of Cerro Colorado involved several episodes of phreatomagmatic eruption and deposition of tuff punctuated by at least two episodes of collapse wherein the inner walls of the tuff cone slumped into a vent. The multilobate form of the crater in plan view suggests the existence of three and perhaps four centers of eruption and subsequent collapse (fig. 9). Although the age of the crater is not known, the presence of Hohokam potsherds on erosion surfaces bevelling the tuff deposits indicates that Cerro Colorado is at least 1,000 years old and supports an age more on the order of 10,000 years (Shakel and Harris, 1972).

Cerro Colorado is different from Crater Elegante in many respects. The tuff beds near the high point of the crater rim dip much more steeply (20-25°) than those of Elegante. These beds are much thicker and in many places the original crater rim is preserved. Indeed, individual beds can be traced from the crater floor up and over the rim to the distal outer flanks where they are buried by alluvium.

The tuff of Cerro Colorado is rich in vesicular, slightly palagonitized, juvenile lapilli and ash together with very abundant accidental ejecta consisting of quartzofeldspathic sand and gravel. Accretionary lapilli are common, especially within the youngest unit of tuff, which underlies the rim of the crater here on its northern side. Note the remarkable lateral continuity of these tuff layers. Many of the uppermost beds are normally graded suggesting an airfall origin for these layers.

Return toward cars and thence to outer slopes of the tuff cone south of the cars.

STOP 3. Surface features of the proximal pyroclastic surge beds. Ejecta in surge beds at this location were blasted up over a collapsed crater rim from the small vent to the southeast. Near the rim, the beds are even and flat, but within about 15 m from the present rim, longitudinal wave forms appear (fig. 10). The longitudinal dunes continue for about 30 m down slope where they give way to a broad, arching transverse dune. Small-scale features, such as ripple marks on the longitudinal dunes, are remarkably well-preserved. These longitudinal dunes have a wave length of about 6 m and a wave height of 50 cm, yielding a height-to-length ratio of 1:12. Such features have not been previously described at any other volcano, although radial gullies are common.

Blanketing the dune horizon are normally-graded, pyroclastic-fall beds. This good marker horizon is locally stripped away.

If time permits we will proceed to the crater floor.

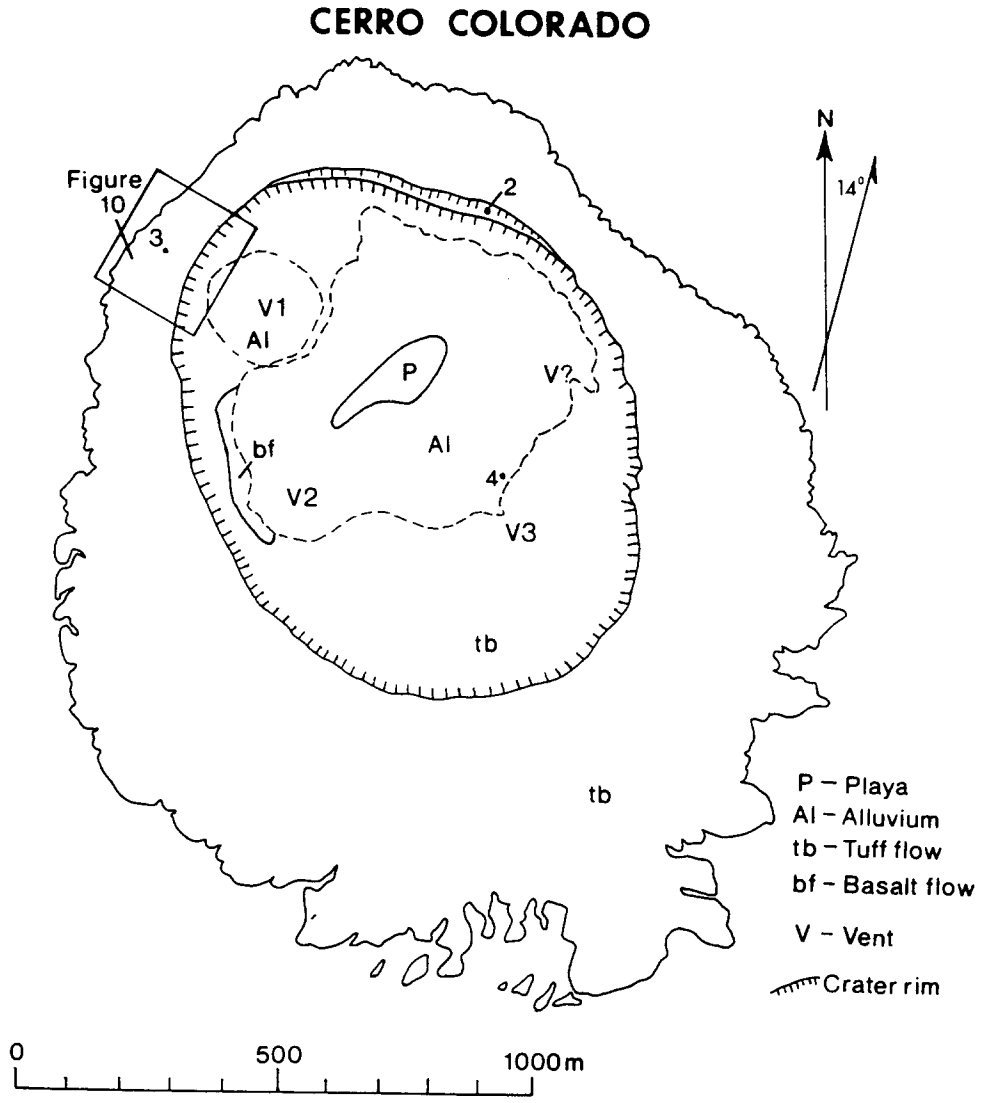

Figure 9. Sketch map of Cerro Colorado. Major units indicated by key. Stops for day 3 given by numerals. (Simplified from Jahns, 1959.)

STOP 4. Inward dipping beds. Associated with the several vents are inward-dipping beds whose bedding planes define portions of downward-pointing funnels. The funnel-like structures converge toward an apex that marks the vent location. These beds apparently represent an explosive phase of eruption following collapse. Vertical crater walls are unconformably overlain by these inward-dipping beds. In a few places, collapse cut the inward dipping beds.

One of the most remarkable features of these beds are the giant sandwave bedforms that make colossal climbing ripples. These forms are best seen in the vincinity of **STOP 4** in figure 9.

Return to cars and to Tempe.

0.4	14.5	Road junction. Bear right.
0.3	14.8	Road junction. Fork left.
3.1	17.9	Road junction. Bear right.
3.8	21.7	Junction with Mexico Rte. 2. Turn right (east).
31.6	53.3	Town of Sonoyta. Turn left toward international border.
2.0	55.3	International border at Lukeville, Arizona. Return to Tempe.

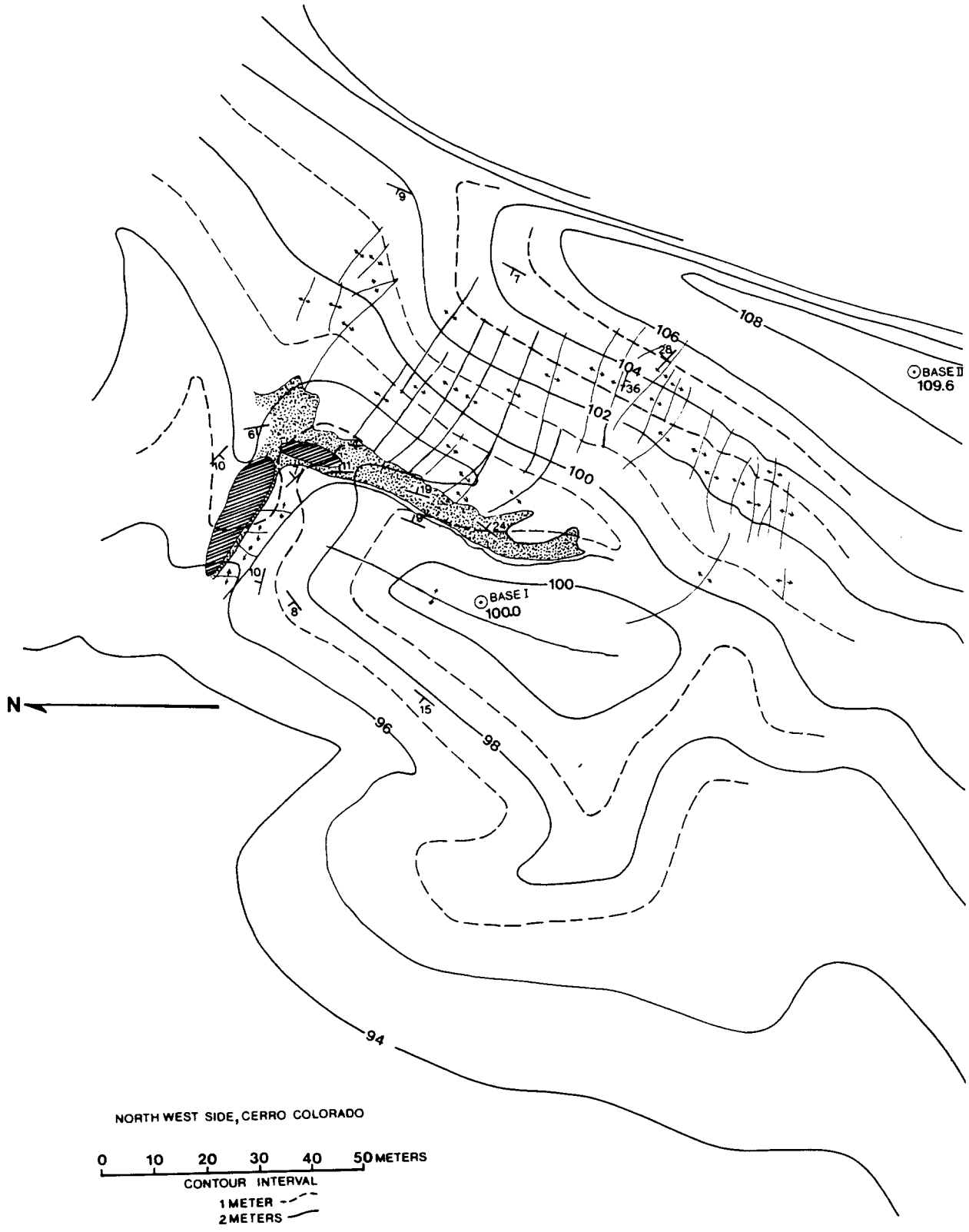

Figure 10. Map of radial dunes at Cerro Colorado. Location of diagram shown in Fig. 9. Contour elevations are relative. Lined and stippled patterns both show air-fall deposits that rest on surge beds. Dune crests indicated by lines with small arrows.

Volcanic Structures and Alkaline Rocks in the Pinacate Volcanic Field of Sonora, Mexico

Daniel J. Lynch II
Laboratory of Isotope Geochemistry
Department of Geosciences
University of Arizona
Tucson, Arizona 85721

James T. Gutmann
Department of Earth and Environmental Sciences
Wesleyan University
Middletown, Connecticut 06457

INTRODUCTION

Pinacate is a typical continental alkali basalt cinder-cone field (Figure 1) that has an exceptionally diverse assemblage of volcanic landforms. Two alkalic rock series make up the field; one constitutes the more than 500 Pinacate monogenetic volcanoes and the other forms the Santa Clara composite volcanic mountain. The purpose of this field trip is to examine some of the landforms and structures and the rocks of which they are made. The first full day entails a climb to the top of the Santa Clara trachyte shield volcano for a view of the entire volcanic field and the surrounding desert. The second day involves transit to Crater Elegante maar volcano and a hike part way into its interior where normally hidden volcanic features are exposed in the walls. Day three will include visits to the intriguing Tecolote cinder cone and to the Cerro Colorado tuff cone.

Volcanoes have been active sporadically here for the past 2-3 million years (Lynch, 1981). Santa Clara rock ages range from 1.7 ± 0.1 to 1.1 ± 0.1 Ma; volcanism on the shield is extinct. The Pinacate monogenetic basalt-hawaiite volcanism began earlier than 1.2 Ma and is only dormant. Volcanism in Pinacate has been coeval with generation of sea-floor basalt at spreading centers in the nearby Gulf of California, but there is no obvious link between them.

The rocks of Volcan Santa Clara constitute an entire alkaline differentiation series. Basalt, hawaiite, mugearite, benmoreite, and trachyte occur in that stratigraphic order. Compositions of olivine, clinopyroxene, Ti-magnetite, and plagioclase found in gabbro nodules dredged up by Pinacate cinder-cone eruptions on the Santa Clara summit can be subtracted in magma-mixing programs to show the possible derivation of the successive rock compositions.

Santa Clara appears to have been derived from a large batch of magma as it differentiated mainly by fractional crystallization, producing a series of eruptions through a central conduit system. The magma body was tapped at various stages in its history to yield the Santa Clara series of alkaline rocks in nearly ideal stratigraphic order.

Basalts and hawaiites of the Pinacate monogenetic volcanoes mantle most of Santa Clara and extend out into the surrounding desert. The Pinacate rocks are typically porphyritic; many contain conspicuously large megacrysts of labradorite, augite, and olivine. Their compositions form tighter groupings on variation diagrams (Figure 2) than do those of the Santa Clara rocks. Each Pinacate cone may represent eruption from one of hundreds of discrete, small magma bodies that formed at different times and places beneath the field.

Pinacate lacks well-defined cone-group alignments. Although the long axis of the field is north-south and the majority of eruptive centers lie within 8 km either side of this axis, cone placement appears to be random.

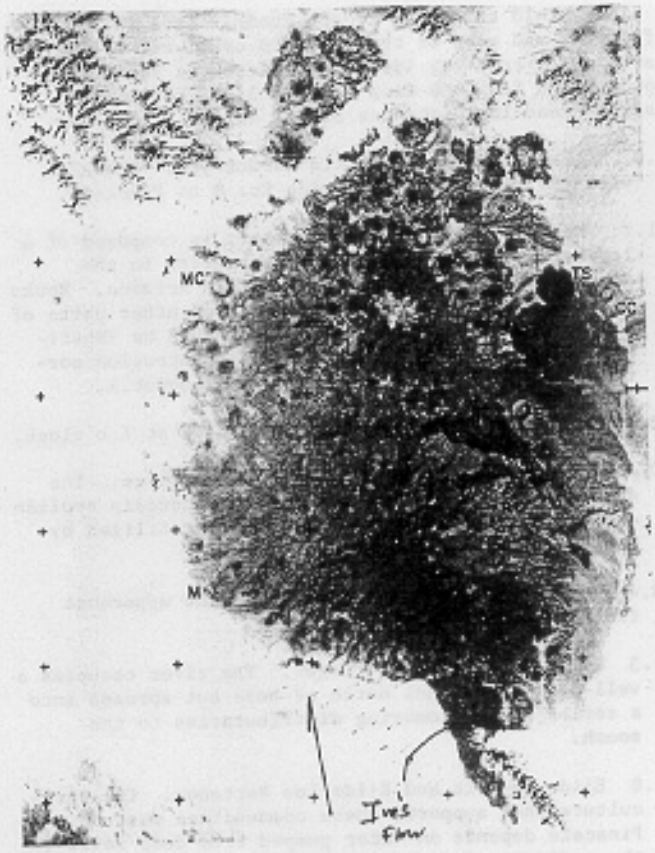

FIGURE 1. PINACATE FROM EARTH ORBIT. Lighter tones near "P" are rocks of Volcan Santa Clara. I- Ives flow, M- Moon Crater, P- Pinacate Peak, RC- Red Cone Camp, E- Crater Elegante, TC- Tecolote, CC- Cerro Colorado, TS- Tesontle, MC- MacDougal Maar. North arrow is 10 km long. Image courtesy NASA.

Cuevo Labortina Lava (Tube)
39°N 55' 5"
80°W 18'
Lava Labyrinth Cave

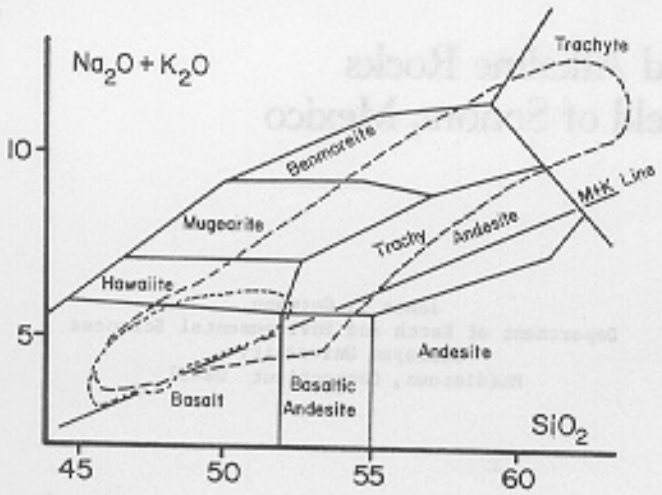

FIGURE 2. ALKALI-SILICA DIAGRAM OF PINACATE VOLCANIC FIELD ROCKS. Long dashes surround the compositional field of Santa Clara rocks, short dashes enclose rocks of Pinacate monogenetic volcanoes. Rock names from LeBas and others (1986), data from Lynch (1981 and unpub.), some Pinacate analyses from Donnelly (1974).

ACCESS TO PINACATE

This field trip will depart Phoenix late in the afternoon and most of the drive to camp will be in the dark. This road log identifying features between Sonoyta and Red Cone Camp (Figure 3) is for later users. Road-log distances are in miles.

0.0 Highway 2 bridge over Rio de Sonoyta. Check in with the ranger before taking Rt. 8 to Pinacate.

11.1 The Sierra Cipriano on the left is composed of a leucogranite apophysis of the batholith in the aerial gunnery range of southwestern Arizona. Rocks collected at this site and in various other parts of the batholith yield K-Ar ages around 53 Ma (Shafiqullah and others, 1980), an age of intrusion corroborated by Rb-Sr isochrons (Damon, unpub.).

13.0 The shield of Volcan Santa Clara is at 2 o'clock.

20.4 North end of the Sierra de San Francisco. The dunes on both sides of the road here contain aeolian dust from the far side of Pinacate, stabilized by desert plants.

25.4 Road to Micro-ondas San Pedro. The uppermost flow has an age of 12.6 ± 0.3 Ma.

31.3 Rio de Sonoyta - 2 bridges. The river occupies a well-defined channel north of here but spreads into a series of anastomosing distributaries to the south.

31.8 Ejido Mayarit and Ejido Los Nortenos. The agriculture that supports these communities east of Pinacate depends on water pumped from deep wells in the sediment of the valleys. The paved road goes on to Puerto Peñasco. Turn north onto the dirt "East Side" road. This road connects with Highway 2 at "El Pinacate" 30 miles west of Sonoyta.

32.1 Road fork, bear left.

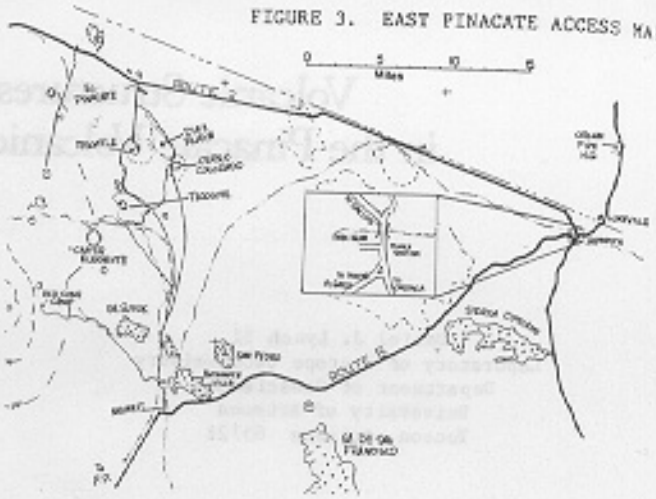

FIGURE 3. EAST PINACATE ACCESS MAP

33.5 Outcrop of Mid-Tertiary basalt possibly contemporaneous with the basalt of Micro-ondas San Pedro. "Diaz Wash," the main drainage for northeastern Pinacate, lies at its western end. This wash never joins with Rio de Sonoyta.

33.7 Cross the wash.

33.8 Summit road intersection, turn west. Drive directly toward the mountain; do not make any major turns until you are on a lava surface.

34.5 West edge of basalt flow designated #452 on Donnelly's (1974) geologic map.

38.5 Road intersection at a large ironwood tree; turn right, up the wash. The road follows segments of wash from here to the lava flow, and it can be wiped out by heavy runoff. It may be necessary to walk to the lava flow on the north, find the road there, and backtrack to your vehicle.

38.9 Edge of the lava north of the wash.

40.0 Cross a deep, possibly soft, 5-m-wide wash.

46.6 Red Cone, the base camp. An alluvial fan of Carnegie cinder here provides a comfortable place to sleep. Scramble up the cone or the flow edge to see a spectacular panorama; the best time is just after sunrise. Pinacate Peak can't be seen from camp.

DAY 1 - HIKE TO THE SUMMIT

Pinacate Peak, a cinder cone on the top of Volcan Santa Clara, can be reached in about 5 hours from Red Cone Camp. Direct hiking distance is 6 km with a total elevation gain of 780 m (2500 ft) from the campsite to the summit. This direct route, which passes many key outcrops of the Santa Clara rock series, is almost entirely on lavas and cinder of the young Carnegie volcano. The hike is not easy; most steep hillslopes are loose soft cinder and many slabs on the young lava surfaces are precariously balanced. WARNING: 2 liters of water may be barely enough if the day gets hot!

Climb up the road ramp in the cliff above the fan, follow the road about 50 m, cross the wash, and climb south onto the edge of the lava flow. Find a convenient place to view the flank of the mountain.

FIGURE 4. EAST FLANK PANORAMA. A slope break between "lower" and "upper" Santa Clara (foreground) occurs on both east and west flanks of the mountain. "DU" numbers are from Donnelly's (1974) geologic map. Drawn from photographs by DJL.

Stop 1

Two major elements of Pinacate geology are obvious (Figure 4): the shield massif of Volcan Santa Clara, and the young lavas and tephra from Carnegie cone, the highest point on the horizon.

The camp at Red Cone is on "Lower Santa Clara," which extends from the desert floor at 150-m altitude to the slope break ahead at 500 m. Its slopes constitute a piedmont to the steeper and more deeply dissected "Upper Santa Clara." Santa Clara flow units dip less than 10^0, a principal characteristic of the trachyte shield volcano type (Webb and Weaver, 1976). Note the difficulty of tracing individual rock units across the face of the mountain from ridge to ridge.

The same deep erosion that presently cuts the mountain flanks existed during the construction of Santa Clara; lavas flowed down canyons, creating geometrically complex contacts between units. As an example, a trachyte of 1.14 ± 0.03 Ma age crops out on the piedmont in the foreground, topographically below outcrops of the oldest exposed members of the series.

Erosion appears to be slow. The mountain flank to the south is covered with Donnelly's unit 42, a basalt of 0.87 ± 0.03 Ma age (Figures 5 and 6). The topography beneath this flow is preserved and has not changed in that considerable period of time.

Carnegie volcano sits atop the western end of a 2-km-long, N70W fissure, the source of several basalt flows. The extensive cinder blanket that covers the summit platform and extends down the northern and eastern flanks of Santa Clara appears to have originated at Carnegie (Figure 5). The three flows that extruded after the main cone-building phase of eruption cross this cinder and are not covered by it. These flows have both aa and pahoehoe surface structures that are described at the next few stops.

The relationships between flow units shown in Figure 5 are complex. The youngest rocks are the darkest. The flow from the "Pahoehoe Jungle" vent (Stop 2) forms the prominent broad lava fall on the flank (left). A separate dark flow extends out from the mouth of Lava Fall Canyon in the distance (our next goal). These two flow units coalesced on the piedmont and poured into

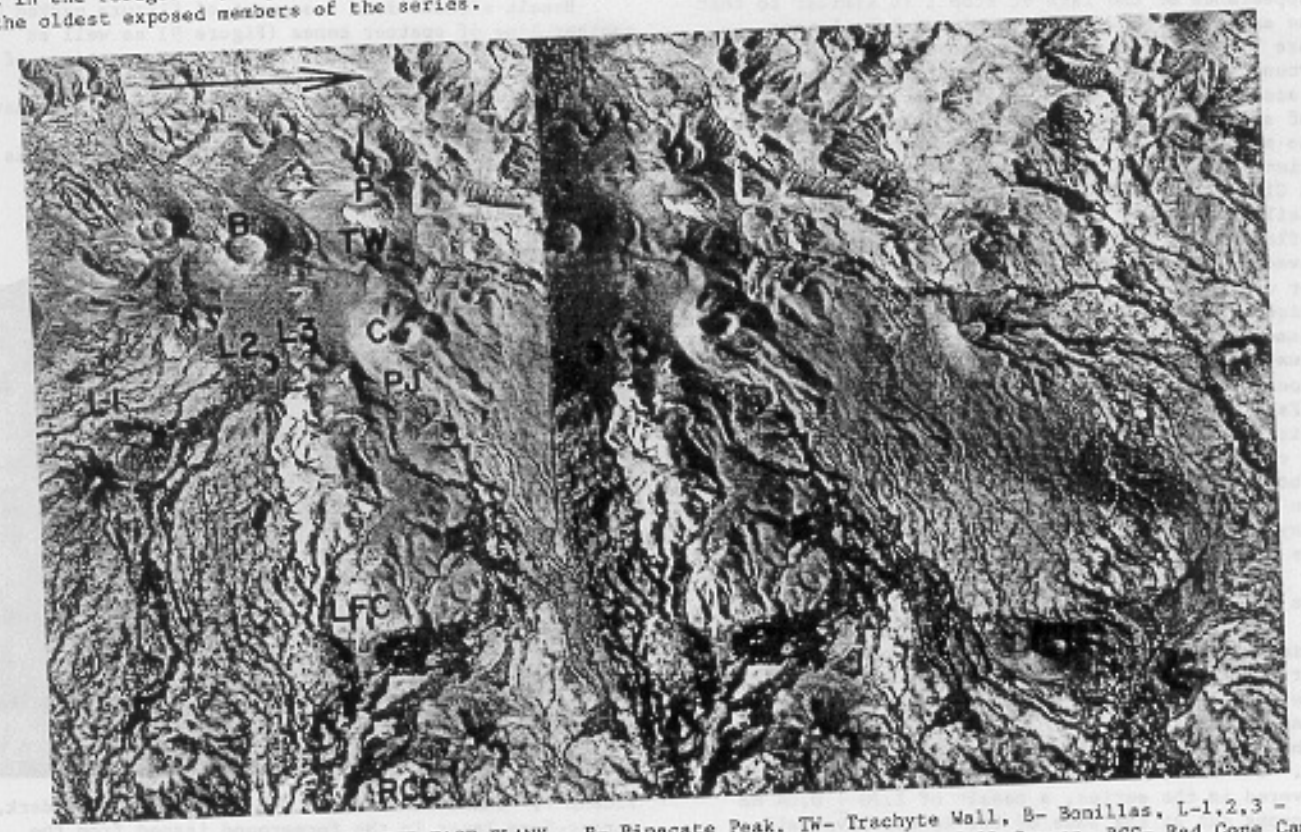

FIGURE 5. STEREO PHOTOGRAPH OF THE EAST FLANK. P- Pinacate Peak, TW- Trachyte Wall, B- Bonillas, L-1,2,3 - Vents on the Lumholtz N20W fissure, C- Carnegie, PJ- pahoehoe jungle, LFC- Lava Fall Canyon, RCC- Red Cone Camp. Distribution of cinder around the summit area, including the NNE feather, is obvious. North arrow is 2 km long.

FIGURE 6. SOUTHEAST FLANK OF VOLCAN SANTA CLARA. Santa Clara rocks are the lightest tones (top right). The gray lava below them is DU 42, which mantled the topography 0.87 ± .03 Ma. Three vents on the Lumholtz fissure are visible at the source of the youngest (darkest) lavas; a fourth vent is just out of the picture on the lower left.

an arroyo cut in lower Santa Clara. The magma, insulated by the arroyo walls, was able to flow an additional 10 km out to the desert floor. Another dark unit from the west base of Carnegie extends west and north, 7 km down an arroyo.

The basalt at Stop 1 is gray in Figure 5 and appears on close examination to be more weathered than the darker basalt; points and corners are not as sharp. The appearance of the lava at stop 1 is similar to that of the extensive flows with prominent lava levees (Figure 7) that also seem to have come from Carnegie. Unfortunately, neither the black nor the gray lavas have accumulated sufficient aeolian material to permit use of soil development as a clue to relative age.

The north wall of Carnegie collapsed during the eruption in a debris-flow avalanche down the flank of Santa Clara (Figure 7) and was then partially rebuilt. The failure occurred directly above the lava-leveed gray flow units, suggesting that they might have been involved. Cone-wall breachment is common in Pinacate cinder cones (Gutmann, 1979), but this debris avalanche is unique. If the gray flows are older than Carnegie and came possibly from Bonillas cone to the southwest, the juxtaposition is coincidental.

Choose your own route across the upper piedmont to Lava Fall Canyon. Between this flow and the canyon flow is an alluvial surface littered with hard, pedogenic carbonate and detritus from Santa Clara deposited atop both Carnegie basalt and Santa Clara trachytes. As you walk across nearly any Pinacate land surface, you may notice fragments of phenocrysts that look like pieces of broken glass.

The lava surface at the mouth of Lava Fall Canyon is all accretionary balls, a common aa surface type. A short segment of Indian trail is visible crossing the lava here. Boulders fallen from the walls litter the lava surface and a mound of alluvial detritus covers the center of the flow in the lower part of the canyon.

The south canyon wall contains three Santa Clara units. The oldest and most primitive rock so far discovered in the series, a basalt of 1.70 ± 0.04 Ma age, crops out at the base of the lowest lava fall. The massive flow unit above it is a mugearite of 1.45 ± 0.03 Ma age. Above that, the ridge-crest unit is a trachyte of 1.26 ± 0.03 Ma age. All the dates are from Lynch (1981).

As you climb the young basalt of the lava fall, note the shear structures and the large accretionary balls welded into the slope. The old lava channel is now an abraded runoff chute, an easy place to climb.

A line of spatter cones (Figure 8) was built on the canyon wall where the Carnegie fissure intersected the surface. The considerable flow of basalt that effused from this vent can be traced onto the piedmont to a place about 1.5 km from the canyon mouth where it coalesced with the flow at lower left in Figure 7.

The best route from the vents is up the opposite (north) side of the canyon, not directly toward Carnegie. Look south from this canyon edge to see the massive trachyte flow/dome that forms the ridge. This is the youngest dated Santa Clara rock with an age of 1.1 ± 0.1 Ma. Climb the cinder-covered slope headed toward Carnegie.

Many Pinacate volcanic units contain megacrysts of labradorite, augite, olivine, and rarely titanomagnetite. The labradorite megacrysts can contain tubular voids up to several millimeters long. These voids are primary inclusions (Gutmann, 1974) representing fluid either exsolved from boundary-layer liquid or, more probably, derived by coalescence of CO_2-rich bubbles. Many phenocrysts in Pinacate lavas were resorbed, whereas many others exhibit skeletal textures. Skeletal morphologies occur among megacrysts more than 1 cm long. The labradorite megacrysts typically are rounded by resorption, but others are perfectly euhedral and riddled with inclusions of basaltic glass. Pinacate megacrysts evidently have various histories. You may find megacrysts in the cinders between here and the peak and in many other places in Pinacate.

Stop 2 - The Pahoehoe Jungle

Basalt effused from a segment of fissure marked by another line of spatter cones (Figure 9) as well as from the side of the cone. Discontinuous sections of lava-tube cave are open through apertures that are rimmed with smooth pahoehoe spatter. Some of them have large bee nests under lava slabs. The stop is at "Iitoi's Cave," a place of worship for the indigenous peoples until the 1930's (Ives, 1942). The trail encountered lower down leads to this place.

FIGURE 7. CARNEGIE CONE AND THE LAVA FALL. The dark, cinder-free lavas in the foreground issued from the fissure at the east cone base. Adjacent on the right are the cinder-covered flows with the prominent lava levees that may have contributed to failure of the cone wall in the prominent debris flow.

Unusual features that Lynch (1981) called "pahoehoe spatter tubes" extend down the sides of some hornitoes. Small blobs of magma spattered off the surfaces of narrow streams flowing down the flanks of the hornitoes and welded to form thin, parallel walls on the sides of the streams. The walls built upward and some joined overhead to enclose the tubes. Similar structures are found on the Ives and Baroque flows.

The route from here is northwest, around the base of Carnegie over the debris flow. Climb diagonally to the right, up the cinder wall above the pahoehoe. Move westward atop the debris flow toward the opposite steep cone wall. On reaching the western edge of the debris flow, traverse across the slope of the cone, climbing slightly upward along the developing trail. Go through the pass to the complex fissure-vent source of the Carnegie-west lava at the west base of the cone wall (Figure 10). You will find superb slab-chaos pahoehoe above the slope break where this flow tumbled over the lip of the hill, changing to aa. Follow the wash westward toward the saddle north of the peak cone. It looks high because you have 220 m more to climb.

Ascent is easier hopping across the boulders on the north side of the valley rather than by slogging through the cinder on the south. On the ridge crest above, flow laminations in trachyte change dip from vertical to horizontal. This ridge might be on the north side of a main Santa Clara vent. The crystalline rock of this wall grades into vitrophyre on Big Horn Ram Ridge to the north.

Climb toward the summit after reaching the saddle. This part of Pinacate Peak cone is littered with gabbro nodules that are probably fragments of the cumulate that resulted from fractional crystallization in the Santa Clara magma body (Lynch, 1981).

Stop 3 - The Summit

At your feet are the more than 500 cinder-cone volcanoes of Pinacate (Figure 11). The range of their ages is obvious from the widely differing erosional morphologies they display. North is toward the prominent contact between the light "Gunnery Range" granite and dark Precambrian rocks of the Sierra Pinta (actual azimuth 359) 60 km away. Below that is the sand belt of MacDougal Pass (25-30 km), which separates the northern section of the field in Arizona from the main part in Sonora. Baboquivari Peak, 180 km due east of

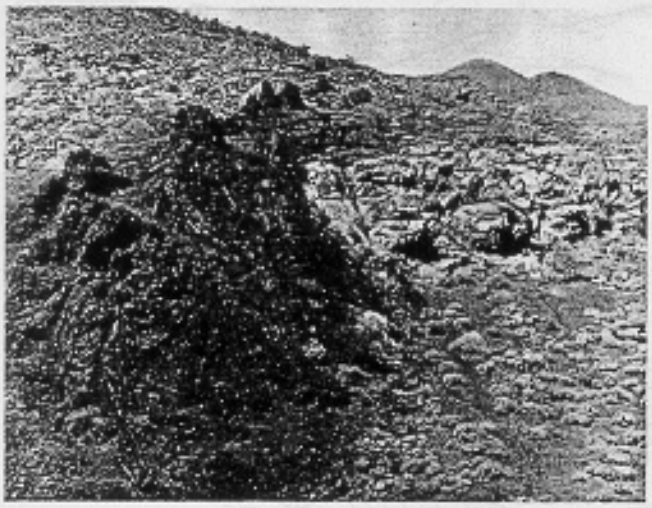

FIGURE 8. SPATTER CONES EAST OF CARNEGIE. A 25-m-long fissure was the source of DU 517. These spatter cones have a wealth of pahoehoe vent features. DJL

FIGURE 9. SOUTHEAST BASE OF CARNEGIE VOLCANO. Thick deposits of cinder lie atop the lava-levees and another fresh flow apparently from Carnegie (lower right). The route down is through the pass on the left of the cone.

Pinacate Peak, can be seen to the right of Carnegie summit only on the best of days. The black area out on the desert flat above the Lumholtz cones is the distal end of the Carnegie flow. The adjacent white area is sediment it has impounded.

The Lumholtz cones, about 1500 m distant on the east edge of the summit platform, are two of four vents on a 1200-m, N20W fissure. These cones are of the same erosional state as Carnegie but appear to be older because Carnegie cinder lies on their lavas (Figure 6).

Ives (1966) reconstructed Kino's travels and reported that he or his companion Manje claimed to have seen the Colorado-Gila River junction from some point in the field and to have determined from this observation that Baja California is not an island. The river junction is 142 km from the summit on the same azimuth as La Jarapena and behind the Sierra del Viejo, neither visible from here nor from the Hornaday Mountains, Ives' deduced location of Manje's vantage point. The mouth of the Colorado River is 133 km from the summit, exactly on the horizon. Kino thought he could see these things, but the geometry precludes it.

Back Down The Hill

The easiest path off the summit is toward the south; aim first for the summit of Bonillas cone and curve left while descending. This avoids the upper parts of the Trachyte wall making the descent a quick, easy cinder slide. The direct route down is eastward, up across the ridge that extends between the "cliffy," eroded cone (0.41 ± 0.04 Ma age) and Bonillas cone. Bear sharply to the left after reaching the saddle, going toward Carnegie, to avoid crossing a cholla-choked cinder flat. Leave the summit platform through the pass east of Carnegie cone.

If time and ambition permit, Carnegie cone can be climbed from the west by ascending the north ridge, thence directly up the side of Carnegie. Getting off Carnegie is the same in any direction, loose and dangerous. Alternatively, one may climb the slopes of Bonillas for a view into its crater or go to the top of the closest Lumholtz cone.

FIGURE 10. BIG HORN RAM RIDGE AND WEST CARNEGIE. The west Carnegie flow may have come from the fissure or from beneath the cinder wall; a mound of tephra lies atop its proximal end. The prominent ridge top is a vitrophyre, the most evolved Santa Clara lava, that rests atop an agglomerate wedge. The horizontal unit beneath it is a benmoreite of 1.15 ± 0.03 Ma age.

The pass leads down to the hornito chain at the fissure above the Pahoehoe Jungle (Figure 8). Cross the lava there and follow its south edge into the canyon. The agglutinate rim cliff above Red Cone can be seen from high in this canyon. Use that, Sierra Suvuk, and the Batamote Hills as guides to find camp. Descend the series of slopes and benches; stay out of canyon bottoms below the highest bench. You will be able to see the lava chaos on the upper piedmont from the top of the last slope and you can adjust your route to avoid crossing it if you so desire.

==========

DAY 2 - TO CRATER ELEGANTE

46.6 From Red Cone Camp, return to Diaz Wash.

59.4 Diaz Wash intersection; turn left (north).

60.0 Chain-fruit cholla forest.

63.1 Bear left at fork; straight is to Cerro Colorado.

66.3 Bear left at fork; straight is to Tecolote.

67.0 "Seniplaya," an extensive area of anastomosing distributary channels in a creosote flat on Salvatierra Wash.

68.9 Dos Mujeres cones on the left.

72.0 Intersection at Salvatierra Wash crossing - continue straight ahead.

73.3 Elegante parking area. Walk to the rim.

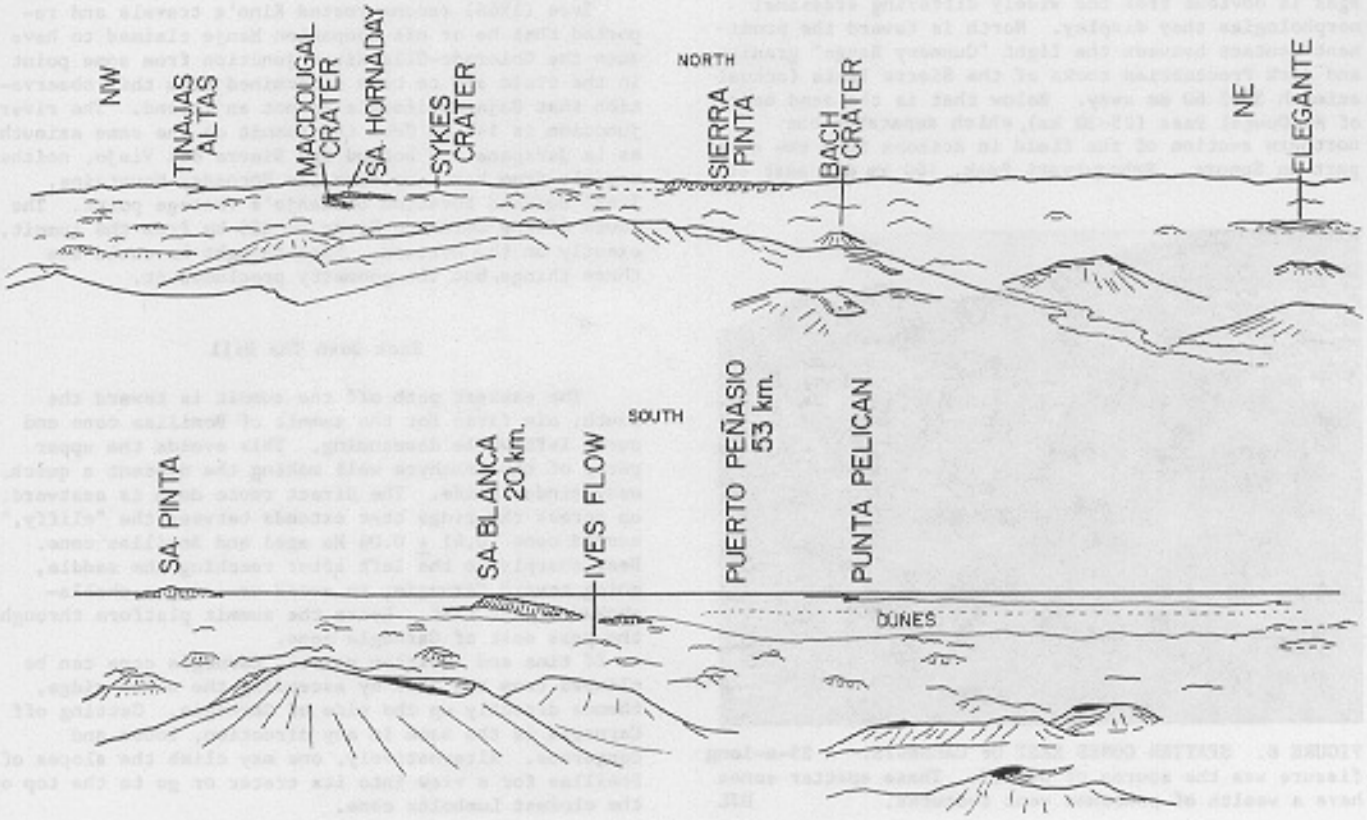

FIGURE 11. PANORAMIC DIAGRAM OF THE PINACATE VOLCANIC FIELD FROM THE SUMMIT. Drawn from photographs by DJL.

Stop 1 - Crater Elegante

Crater Elegante (Figure 12) is the largest of nine maars in Pinacate. It is 1600 m in diameter and 244 m deep. Gutmann (1976) described the geology of Crater Elegante and included geologic maps of the crater and of its walls; copies will be distributed to participants. The crater originated by collapse attendant upon hydromagnatic eruptions that deposited tuff breccia from pyroclastic-surge clouds.

The oldest lava flow exposed in the crater wall is a hawaiite of 0.5 ± 0.1 Ma age (all dates from Lynch, 1981). This flow and others above it come from unknown sources. Upon these is a flow from the largely buried cinder cone just south of the crater. Cinders from that cone appear in the southern crater walls resting on this flow, deformed by its motion, and overlain by similar, younger flows.

The cinder cone displayed in cross section in the eastern and southern walls of the crater (far wall in Figure 12) is above these flows. Two units from this cone yield K-Ar ages of 0.46 ± 0.05 and 0.43 ± 0.06 Ma. Up-dip projections of its layering indicate that its principal vent lay in the southeastern part of the maar, about where the floor meets the foot of the talus. The first unit erupted from this vent was a flow that baked and/or deformed the overlying cinders. This cone was breached on the southeast following emplacement of sills within the cone and along its base. Renewed eruptions then produced phenocryst-rich cinders, flows, and dikes.

Several more volcanic units were erupted prior to the cataclysmic eruption that produced the maar. A thick dike fed a shallow, sill-like intrusion and small flows (unit dp of Gutmann, 1976, Figure 3) that rest on the crystal-rich cinders in the breach of the cone. In the southeastern wall of the crater, a dike fed a tiny cinder cone with a lobate sill at its base.

Resting on these are younger cinders from a cone centered in the southern part of what is now the maar. Like their predecessors, these cinder eruptions were immediately preceded by effusion of a lava flow.

The maar-forming eruption began with effusion of a lava flow from a vent probably located near or somewhat northeast of the center of the crater. The age of this flow is 0.15 ± 0.02 Ma. Minor eruption of cinder may have followed this, but groundwater soon gained access to the conduit and the hydromagnatic eruptions began.

Chief constituents of the tuff breccia at the crater rim are vesicular pellets of glassy, juvenile ash rich in tiny crystals, accessory blocks of basalt torn from the vent walls, and quartzofeldspathic sand, silt, and clay from beneath the volcanic section. Accessory ejecta decrease rapidly in abundance with distance from the crater rim, whereas the abundance of silt and clay increases in that direction.

Unless the space into which collapse occurred was made by evacuation of a shallow magma chamber, the volume of ejecta originally deposited outside the crater must be at least as great as the volume of missing material. Thickness variation of the tuff breccia with distance from the rim indicates that ejecta equal to about one-third of crater volume were deposited between the rim and 1.3 km away from the rim. The trends of compositional change out to 1.3 km indicate that the distal parts of the deposit were chiefly fine-grained sediment and that this sediment was by far the most abundant constituent ejected from the crater. Evidently, the space into which collapse occurred was made chiefly by ejection of large quantities of unconsolidated sediment from beneath the volcanic section.

The estimated volume of accessory ejecta between the crater rim and 1.3 km away is 9 percent of the volume of the crater below the base of the tuff breccia. The tuff breccia contains abundant blocks petrographically unlike rocks exposed in the crater walls,

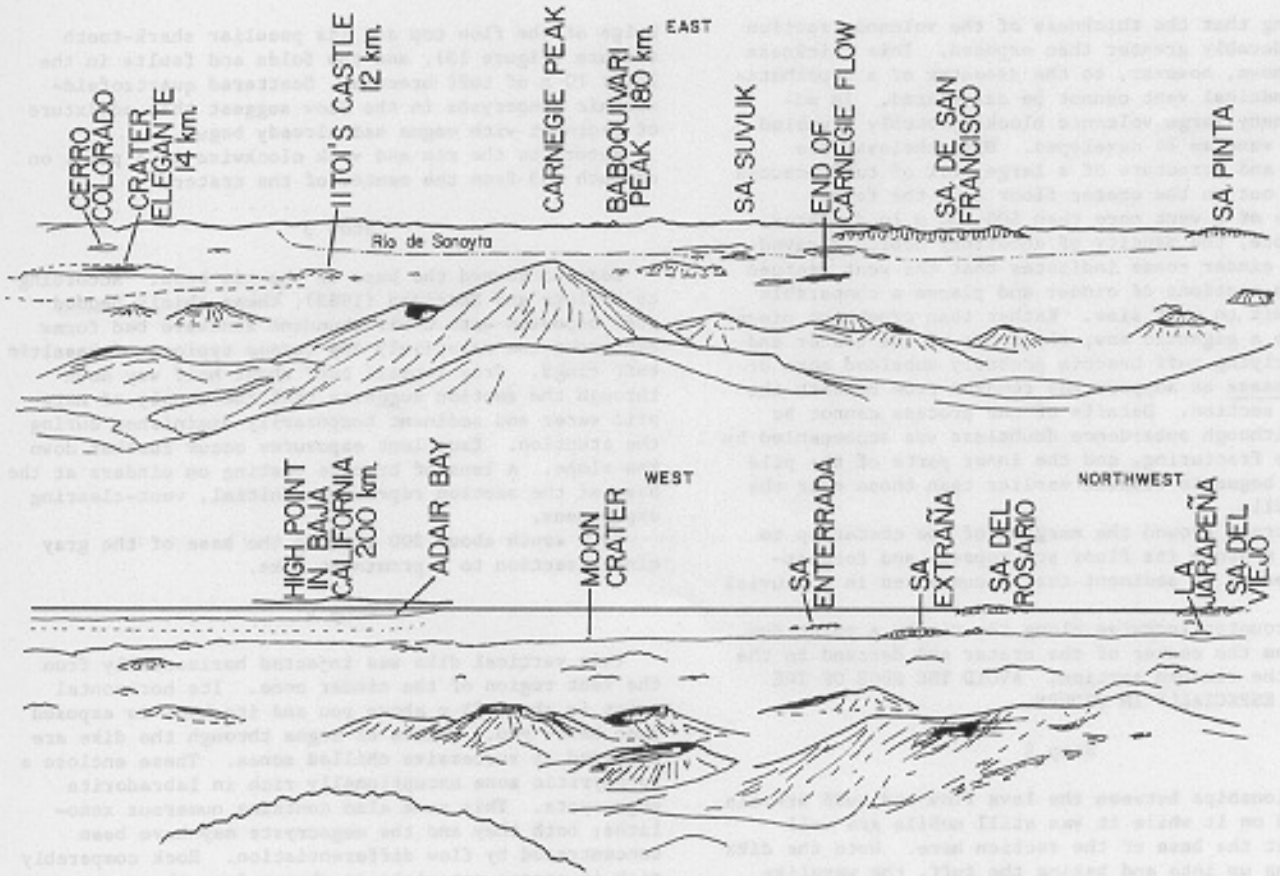

FIGURE 12. CRATER ELEGANTE FROM THE WEST. The blanket of tuff breccia forming the rim of the collapse depression partly buried the old cone on the right edge of the photo. Strata from that cone and two others are exposed in the crater walls. Salvatierra Wash is in the upper left.

suggesting that the thickness of the volcanic section is considerably greater than exposed. This thickness is not known, however, so the diameter of a hypothetical cylindrical vent cannot be calculated. In addition, many large volcanic blocks probably crumbled into the vent as it developed. Nevertheless, the position and structure of a large hill of tuff breccia cropping out on the crater floor deny the former existence of a vent more than 600–700 m in diameter. Furthermore, the paucity of accessory debris derived from the cinder cones indicates that the vent pierced only thin sections of cinder and places a comparable upper limit on vent size. Rather than crumbling piecemeal into a gigantic maw, the rocks of the crater and much overlying tuff breccia probably subsided more or less en masse as support was removed from beneath the volcanic section. Details of the process cannot be known, although subsidence doubtless was accompanied by extensive fracturing, and the inner parts of the pile may have begun to subside earlier than those near the crater walls.

The strata around the margins of the crater up to about 60 m above its floor are topset- and foreset-like deposits of sediment that accumulated in a pluvial lake.

Walk counterclockwise along the rim to a point due north from the center of the crater and descend to the base of the rim-bed section. AVOID THE EDGE OF THE CLIFFS – ESPECIALLY IN GROUPS.

Stop 2

Relationships between the lava flow and tuff breccia deposited on it while it was still mobile are well exposed at the base of the section here. Note the dike projecting up into and baking the tuff, the wavelike bulge of the flow top and its peculiar shark-tooth texture (Figure 13), and the folds and faults in the lower 10 m of tuff breccia. Scattered quartzofeldspathic xenocrysts in the flow suggest that admixture of sediment with magma had already begun.

Return to the rim and walk clockwise to a point on azimuth 063 from the center of the crater.

Stop 3

Descend toward the base of the rim beds. According to Wohletz and Sheridan (1983), these thinly bedded tuff deposits with their abundant sandwave bed forms represent the relatively dry surges typical of basaltic tuff rings. Gray lapilli tuff about half way down through the section suggests that the supply of meteoric water and sediment temporarily diminished during the eruption. Excellent exposures occur further down the slope. A lens of breccia resting on cinders at the base of the section represents initial, vent-clearing explosions.

Walk south about 200 m along the base of the gray cinder section to a prominent dike.

Stop 4

This vertical dike was injected horizontally from the vent region of the cinder cone. Its horizontal crest is about 33 m above you and its keel is exposed just below you. Pulses of magma through the dike are recorded as successive chilled zones. These enclose a porphyritic zone exceptionally rich in labradorite megacrysts. This zone also contains numerous xenoliths; both they and the megacrysts may have been concentrated by flow differentiation. Rock comparably rich in coarse materials is absent from the upper parts

of the dike. It is possible that gravitational settling contributed to their concentration in the lower part. The core of the dike is occupied by an intrusion of chilled basalt that widens upward. PLEASE DO NOT MINE THE DIKE ANY FURTHER; SAMPLE THE LOOSE ROCKS INSTEAD.

Note the tan, tuffaceous layers in the cinder section here. These contain slightly palagonitized juvenile ash together with accidental sand and silt. They suggest incipient hydromagnatic activity that failed to lead to a major tuff eruption.

Return northward 50 m and ascend the first gully to the upper parts of the dike. These contain sheetlike megavesicles more than 1 m long with magma drips on their walls. The vesicles may be gravity-driven gas accumulations in the top of the dike. Note also the bifurcations of the dike crest in the cinder.

Return to the crater rim and continue clockwise to the edge of the scallop-shaped depression about 100 m beyond the highest point on the crater rim. Note the narrow dike feeding a sill and tiny cinder cone atop the south wall of the crater. Descend gradually into the Scallop to the upper parts of the cinder section on a 110° azimuth from the center of the crater (see Gutmann, 1976, Figure 3).

Stop 5

This depression began as a breach in the wall of the cinder cone. Masses of cinder were carried from the breach on a flow exposed on the flats east of the crater. Following breachment, the breach was partially filled as renewed eruptions produced phenocryst-rich, relatively dense bombs. A small flow of similar lava is exposed high in the northeastern part of the Scallop, and another flow occurs outside the crater southeast of the Scallop. Large, gem-quality labradorite crystals occur in these cinders as do rare clinopyroxene megacrysts. Clinopyroxene crystals from this locality as much as 1.8 cm long can exhibit sector zoning.

Return to the rim, continue clockwise to azimuth 167°, and descend through the tuff breccia and underlying cinders to the top of the highest flow.

Stop 6

These gray cinders were derived from a vent located out in what is now the crater. The flow beneath them carries the same phenocryst assemblage and rests on cinders from the old cone to the northeast. Where flow-top breccia is absent, the base of the overlying cinders is oxidized and indurated to form a resistant, red ledge a few centimeters thick. These cinders were baked by the underlying flow, effusion of which must have immediately preceded the cinder production.

Climb down over the flow, traverse a few meters westward, and descend the gully through the older cinders to the top of the cliffs. Exposed in this gully is a dike that is the upturned end of a sill emplaced along the base of the gray cinder cone. The cinders are deformed over the flow at the top of the cliffs here; this flow immediately preceded pyroclastic eruptions and is petrographically identical to a flow that bakes the base of the cinder section in the northern walls of the crater.

Return to the rim, walk back eastward to the 145° azimuth, and turn southward into the gully dissecting the outer slopes of the tuff breccia.

Stop 7

Displayed in the walls of this gully within a few hundred meters from the rim is a variety of pyroclastic-surge bed forms. Wohletz and Sheridan (1979) mapped the transition from sandwave facies through massive beds to planar bed facies progressing outward from the rim in this area. Look for low-angle cross-stratification, soft-sediment deformation features, and deflation structures in the tuff beds.

Return to the rim; walk counterclockwise along the rim to the road and down the road to the new camp.

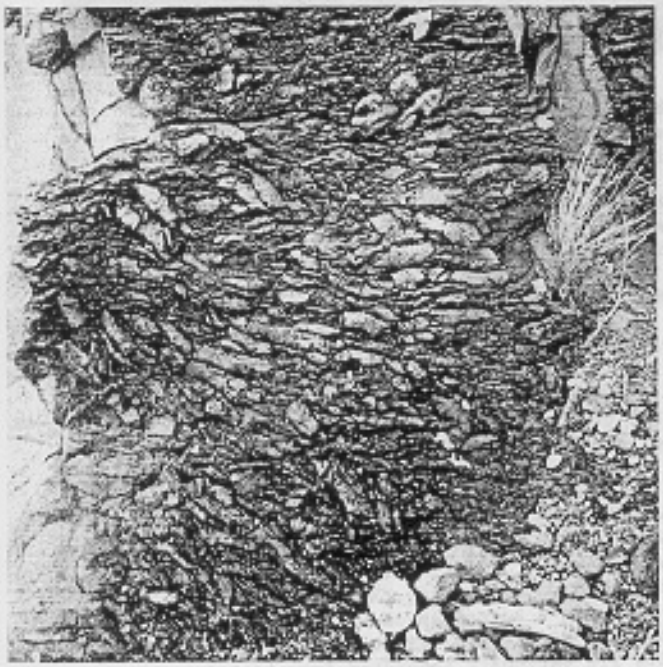

FIGURE 13. SHARK-TOOTH OR CORDUROY TEXTURE. This distinctive texture forms at the interface between fluid basalt and unconsolidated material like fresh tuff breccia or cinder. Grass clump is 15 cm high.

FIGURE 14. TECOLOTE VOLCANO. Flow S blocked Salvatierra Wash (bottom), diverting the water and trapping sediment in the white area on the left. The adjacent black lava appears to have flowed out from under the cinder deposited earlier atop the flow.

FIGURE 15. TECOLOTE FROM THE SOUTH. Mayo cone, slightly older, is 1 km to the north; Tesontle cone, possibly younger, is 5 km beyond that. The arrow points to the "Bus" bomb. Note the faults, the gullies inboard of flows A and B, the valley separating the cinder wedge from the main cone, two collapse depressions on the east rim, and an enigmatic "crater" on the slope in front of flow R (foreground). Peter Kresan copyright 1987.

DAY 3 - TECOLOTE VOLCANO

Tecolote Volcano is one of the youngest cones in Pinacate and is certainly one of the most complex of the small eruptive centers. A wealth of lava surface types and pyroclasts, including bombs of astounding size, are concentrated within its small area - most can be visited in an easy morning walk.

The volcano consists of a complex cone, six lava flows, and a cinder blanket (Figure 14). Contacts between adjacent flow units and between lava and cinder permit development of a crude eruption chronology. Tecolote cinder lies atop Mayo, the adjacent cone on the north, but the aa lavas from each volcano are nearly indistinguishable at their contact.

Tecolote "cone" is not conical. The main edifice is U-shaped and open to the northwest. An irregular group of tephra hills lies west of the south horn, and a wedge-shaped mass of cinder is attached on the southeast. Four of the six Tecolote flows originated from the base of this wedge; flows A, B, and C effused from distinct boccas in its eastern wall. The origin of flow S is not as clear, but at least some of S came from the base of an amphitheater on the southwestern end of the wedge (foreground in Figure 15). Broad cinder blankets extend both northward and southeastward from Tecolote.

The tops of both horns of the cone are cut by arcuate, semiparallel fault scarps that are most numerous on the north horn (clearly visible in Figures 15 and 16). Where the tephra was cemented by fumarolic activity, the scarps are vertical and show downward relative motion of the side nearer the crest. The crest appears to have subsided as a complex graben. No other cone in Pinacate is known to have such faults. Gutmann and Sheridan (1978) described faults at Tesontle cone that they attributed to motion in the underlying lava, but they were cone-flank faults.

Tecolote cone is composed of various tephra types. The wedge appears to be entirely well-sorted, nonindurated cinder. Material exposed in the walls of the interior craters, including the high inner wall of the south horn, is a heterogeneous mixture of cinder, scoria, agglomerate, and agglutinate. The tephra deposits are variously indurated from tightly welded agglutinate, compacted agglomerate to loose material. Similar mixed tephra constitute the mounds of wall material that litter the surface of flow Q.

Most striking is the distinctive layer of large bombs that covers the south and east rims and mantles

the outer southern cone slope. Few are smaller than 20 cm in diameter. Most were spherical but many are broken. Accessory blocks derived from older volcanic units and accidental fragments of quartzofeldspathic rock occur loose in the deposit and also constitute cores in some of these bombs. The juvenile bombs are dense and relatively crystal-rich, with tiny vesicles. Many have cauliflower surfaces; others are more fluidal. These characteristics suggest that the magma was degassed and somewhat stiff and pasty.

The tephra mounds on the west are rich in notably large bombs, many having major axes longer than 1 m. These large bombs are generally spindle shaped with stretch-striated surfaces. The largest found so far is shown in Figure 17.

Cinder blankets extend from Tecolote in two directions. The plume on the north covers and fills a section of the aa surface of flow Q (Figures 14-16), mantles the slopes of Mayo, and extends almost to Tesontle. On the south, flow S is nearly completely covered with cinder and only the distal edges on east and west show more than the ends of flow-top projections. Irregularities in the cinder blanket caused by postdepositional flow within S are visible in Figures 14 and 16. Baked zones of red cinder can be seen in crevasses developed in S and the basal cinder is reddened adjacent to some of the flow-top projections.

Features of the Tecolote Flow Lavas

Aa is the major surface type. Roughness exists on scales ranging from micrometer spines on rock surfaces to meter-tall projections above flow surfaces. Surface blocks range from decimeter to multimeter, irregular to slab, locked in place to precariously balanced. The surface material is usually highly scoriaceous with irregular vesicles. Pahoehoe is present on B at various places starting about 100 m from the bocca.

The A flow is noteworthy in being composed entirely of "anosma," squeeze-ups of viscous magma with scrape and chattermarks attributable to plastic to brittle deformation. Striated slabs project out of fractures in many other Pinacate flow surfaces, but this unit is unusual because the slabs are stacked one against the next like plates in a dishwasher rack (Figure 18). The A flow excavated a canyon in the outer wall of the wedge and its distal end is covered with piles of the cinder it removed.

FIGURE 16. TECOLOTE VOLCANO. This photograph shows the faults, the central craterlets, the tephra mound atop R (lower right) and its near contact with Q, and the assorted tephra mounds atop Q (left and bottom) detached from the cone wall. © - Peter Kresan, 1987.

FIGURE 17. THE "BUS" BOMB. This pyroclast, 4.5 x 3.1 x 2.5 m, is 200 m from the nearest craterlet and 400 m from the center of the cone.

Flow B effused from a bocca on the outer face of the wedge. The B magma appears to have been highly gas-charged and of low viscosity. Some of the surface structures near the B bocca resemble shelly pahoehoe but are, nonetheless, spiny aa. B has dendritic structures (Figure 19) on the edges of some slabs about 100 m east of its vent.

Flow C, the most northerly small flow on the east side of the wedge, emerged from a broadly excavated amphitheatre much like the source of S. A short lava tube near its source is a cool refuge on a hot day. The surface of C near the proximal end is slab aa, much less scoriaceous than the aa of B. For much of its length, C is flanked by a series of cinder "dunes" of unknown origin.

Flow R emerged on the ridge between Tecolote and the older cone to the southwest. This flow split: one tongue spilled eastward down the ridge toward S and the other westward down the ridge toward Q. The exact source of R is not clear; it may have emerged from beneath the closest of the western tephra hills. A mass of tephra was rafted outward along the ridgecrest by R. R and Q did not meet; a space of about 1 m separates the two flow fronts north of the ridge.

Flow Q is the largest and most complex of the Tecolote flows. It can be traced directly to the center of the cone, the presumed main vent. Where not buried beneath tephra, the surface is free-clast aa, slab in some places and irregular in others. To the northwest, Q overlies the edge of a nearly identical aa flow that originated from Mayo.

The surface of Q is littered with debris from the breached cone wall both in clearly defined, blocky masses and in rubbly piles (Figure 16). Tall mounds of bedded tephra are a distinctive feature of Q. The layers of solid basalt seen on the sides of some of these mounds were emplaced as dikes at an acute angle to the bedding when liquid basalt welled into opening fissures as the cone wall failed. The tall mounds of bedded tephra near the eastern distal end are far too large to have been simply rafted along the top of the flow as material is normally transported by aa. They may have slid along a lubricating basalt layer.

FIGURE 18. ANOSMA ON THE "A" FLOW. The bocca of A is in a canyon cut in the cinder of the wedge. People on the right show the size of these large slabs.

Flow Q effused from the center of the crater after having breached the northwest segment of wall. The five other flows emerged from various places beneath the walls. Nearly parallel gullies extend inward from the boccas of A and B across both the wedge and the cone. Another gully extends inward from R through the outer tephra hills. These gullies appear to have been excavated from beneath by block caving of tephra into voids created by removal of the cinder as magma flowed beneath.

A Possible Scenario for the Eruption

Relationships between the geologic features at this exceptionally complex eruptive center do not permit inference of a complete eruption chronology and the origin of many of the features is not understood. Flow S is apparently the oldest flow. Its thick, deformed mantle of locally baked cinder suggests that its effusion immediately preceded most or all of the pyroclastic eruptions that built the central cone. However, at least part of flow S appears to have emerged from an amphitheater at the base of the wedge after the cinders of the wedge had been deposited. It seems possible that the wedge, and perhaps the tephra hills west of the south horn, could be remnants of a cone built just prior to the large central cone.

Effusion of Q was contemporaneous with the last part of construction of the central cone. Flow Q removed a large section of cone wall and carried substantial pieces of it nearly 6 km out onto the desert. The apparently undisturbed band of cinder atop Q suggests that it had stopped moving prior to the end of cinder eruptions at this locality. Some of the giant bombs are on tephra that rest atop Q (Figure 17).

Eruption of large bombs followed all major cinder eruptions and evidently was not accompanied by significant cinder production. The remarkable size of these bombs demands a powerful eruptive force. One possible driving mechanism is a gas jet described as a "gas blast" by Budnikov and others (1983) from the eruption of Gorshkov cone on Tol'bachik. Such a jet entrains large blobs of magma and blocks of wall rock during "throat clearing." The source of the gas is problematic. Eruptions of cinder can have large gas-to-magma ratios, but little if any cinder appears to have accompanied these bombs. Relatively fluidal bombs on the south rim contain more abundant phenocrysts (especially microphenocrysts) than do the earlier, cone-building cinders. Crystallization of vapor-saturated melt held beneath the volcano would have been accompanied by resurgent boiling. Accumulation of the evolved gas beneath a plug of pasty magma could have contributed to high gas/magma ratios; and the volume increase associated with such boiling could have led to cracking of the conduit walls, access of ground water to the system, and consequent hydromagmatic gas production. Whatever the driving mechanism, some of these bombs are of extraordinary size.

The large bombs are absent from the surfaces of flows A and B, but are present on the cinder adjacent to their boccas. Effusion of these small-volume flows appears to have followed the bomb eruption. The bombs on the surface of flow R, also a small-volume unit, could have been carried along after it disaggregated the tephra hill above its source.

Some bombs on the rim have yellowish surfaces altered by fumarolic activity. This activity also cemented tephra of the main cone locally, and the cemented zones are cut by faults of the cone-rim fault system. Also among the last events is formation of the craterlets within the debris on the floor and at the breach of the central crater. Some of these evidently represent local collapse, whereas a few near the breach appear to reflect minor explosions that produced small amounts of relatively crystal-rich scoria. Except for the relationship between the faults and the fumarole-cemented tephra, most of the sequence of events following eruption of flow Q is unclear. The complexity of relationships on Tecolote almost assures a future of lively conjecture.

Return to the vans for the drive to the lunch stop at Cerro Colorado.

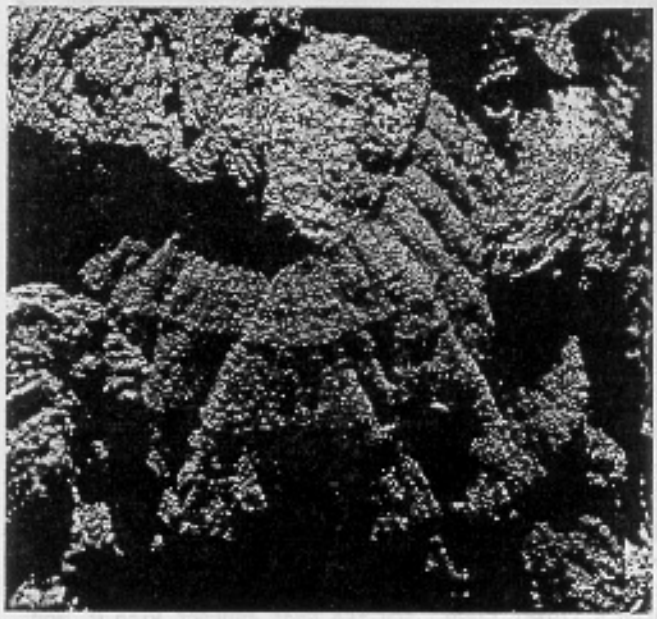

FIGURE 19. DENDRITIC OR ARBORESCENT STRUCTURE ON "B." This structure appears to have grown as two pahoehoe slabs pulled apart.

FIGURE 20. CERRO COLORADO TUFF CONE. This view looks southwest across Cerro Colorado toward the shield of Volcan Santa Clara (top left) and the dunes of the Desierto de Altar beyond Pinacate (top right). Tecolote is directly above the high crest of the tuff cone and Crater Elegante is above and to the left of that. Note the dark, inward-dipping tuff layers on the south wall of the crater, the broad apron of detritus shed from the cone, and abrupt termination of gullies draining its outer slopes. Cerro Colorado blocked a major drainageway creating Diaz Playa, which is out of this view on the right. Peter Kresan copyright 1987.

74.6 Salvatierra Wash Crossing.

77.3 Bear right at the road fork (the left fork passes Mayo and Tesontle cones and exits via the cinder mine road - 9 miles). Bear left at the next fork about 30 m beyond.

81.6 Rim of Cerro Colorado Crater.

Lunch Stop - Cerro Colorado Crater

Cerro Colorado is a reddish tuff cone with a crater about 1000 m in diameter. The cone was mapped by Jahns (1959) and its stratigraphy described by Wohletz and Sheridan (1983). Playa deposits in the northern and eastern walls of the crater are overlain by thin-bedded and then massively bedded surge deposits capped by air-fall tuff. Compared to the rim beds at Elegante, those here are rich in gravel, attain steeper dips, are thicker and more massive, exhibit more palagonitization of juvenile clasts, and contain accretionary lapilli and mud-armored clasts. Cerro Colorado is a tuff cone built by relatively wet pyroclastic surges (Wohletz and Sheridan, 1983). Its form suggests the presence of several centers of eruption and collapse. Its original rim is preserved on the south side where beds can be traced up from the crater floor over collapse-truncated older layers and finally over the rim of the crater. Normally graded air-fall deposits rich in accretionary lapilli are well exposed on the path to the highest point on the north rim of the crater.

Follow the road to the west and north to exit Pinacate.

86.2 Broad cinder-haul road; turn right.

88.0 Highway 2; turn right. Sonoyta is 32 miles away.

ACKNOWLEDGMENTS

Financial support for some of the aerial photography came through a grant to D.J. Lynch from the Tucson Gem and Mineral Society.

Aerial oblique photographs in Figures 15, 16, and 20 are copyrighted by Peter Kresan; all other oblique and ground photographs are by D.J. Lynch.

REFERENCES CITED

Budnikov, V.A., Markhinin, Ye.K., and Ovsyannikov, A.A., 1983, Quantity, distribution and petrochemical features of pyroclasts of the Great Tolbachik Fissure Eruption, in Fedotov, S.A., and Markhinin, Ye.K., eds., The Great Tolbachik fissure eruption: Cambridge, U.K., Cambridge University Press, p. 41-56.

Donnelly, M.F., 1974, Geology of the Sierra del Pinacate volcanic field in northern Sonora, Mexico, and southern Arizona, U.S.A. [Ph.D. thesis]: Stanford, Stanford University, 722 p.

Gutmann, J.T., 1974, Tubular voids within labradorite phenocrysts from Sonora, Mexico: American Mineralogist, v. 59, p. 666-672.

_____ 1976, Geology of Crater Elegante, Sonora, Mexico: Geological Society of America Bulletin, v. 87, p. 1718-1729.

_____ 1979, Structure and eruptive cycle of cinder cones in the Pinacate volcanic field and the controls of Strombolian activity: Journal of Geology, v. 87, p. 448-454.

Gutmann, J.T., and Sheridan, M.F., 1978, Geology of the Pinacate volcanic field, in Peve, T., and Burt, D., eds., Guidebook to the geology of central Arizona: Arizona Bureau of Geology and Mineral Technology Special Paper 2, p. 47-59.

Ives, R.L., 1942, The discovery of Pinacate volcano: The Scientific Monthly, v. 54, p. 230-237.

_____ 1966, Kino's explorations at Pinacate: Journal of Arizona History, v. 7, p. 59-75.

Jahns, R.H., 1959, Collapse depressions of the Pinacate volcanic field, Sonora, Mexico, in Heindl, L.A., ed., Southern Arizona Guidebook II: Arizona Geological Society, p. 165-184.

LeBas, M.J., LeMaitre, R.W., Streckeisen, A., and Zanettin, B., 1986, A chemical classification of volcanic rocks based on the total alkali-silica diagram: Journal of Petrology, v. 27, p 745-750.

Lynch, D.J., 1981, Genesis and geochronology of alkaline volcanism in the Pinacate volcanic field of northwestern Sonora, Mexico [Ph.D. thesis]: Tucson, University of Arizona, 248 p.

Shafiqullah, M., Damon, P.E., Lynch, D.J., Reynolds, S.J., Rehrig, W.A., and Raymond, R.H., 1980, K-Ar geochronology and geologic history of southwestern Arizona and adjacent areas: Arizona Geological Society Digest, v.12, p. 201-260.

Webb, P.K., and Weaver, S.D., 1976, Trachyte shield volcanoes: a new volcanic landform from South Turkana, Kenya: Bulletin Volcanologique, v. 39, p. 294-312.

Wohletz, K.H., and Sheridan, M.F., 1979, A model of pyroclastic surge, in Chapin, C.E., and Elston, W.E., eds., Ash flow tuffs: Geological Society of America Special Paper 180, p. 177-194.

_____ 1983, Hydrovolcanic explosions II; evolution of basaltic tuff rings and tuff cones: American Journal of Science, v. 283, p. 385-413.